NASA TECHNICAL REPORT

NASA TR R-335

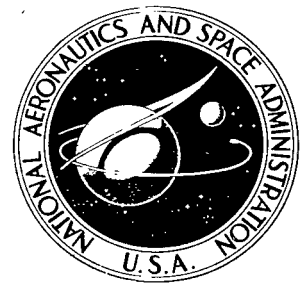

NASA TR R-335

THE ONE-DIMENSIONAL TIME-DEPENDENT INTERACTION OF A SATELLITE WITH THE IONOSPHERIC PLASMA

by Nobie H. Stone and John W. Sheldon

George C. Marshall Space Flight Center
Marshall, Ala.

NATIONAL AERONAUTICS AND SPACE ADMINISTRATION • WASHINGTON, D. C. • APRIL 1970

1. REPORT NO.	2. GOVERNMENT ACCESSION NO.	3. RECIPIENT'S CATALOG NO.
NASA TR R-335		

4. TITLE AND SUBTITLE

The One-Dimensional Time-Dependent Interaction of a Satellite with the Ionospheric Plasma

5. REPORT DATE
April 1970

6. PERFORMING ORGANIZATION CODE

7. AUTHOR(S)
Nobie H. Stone and John W. Sheldon

8. PERFORMING ORGANIZATION REPORT #
M431

9. PERFORMING ORGANIZATION NAME AND ADDRESS

George C. Marshall Space Flight Center
Marshall Space Flight Center, Alabama 35812

10. WORK UNIT NO.
124-09-00-00-62

11. CONTRACT OR GRANT NO.

12. SPONSORING AGENCY NAME AND ADDRESS

National Aeronautics and Space Administration
Washington, D.C 20546

13. TYPE OF REPORT & PERIOD COVERED

Technical Report

14. SPONSORING AGENCY CODE

15. SUPPLEMENTARY NOTES Nobie H. Stone is a physicist with the Space Sciences Laboratory, George C. Marshall Space Flight Center and John W. Sheldon is Associate Professor, School of Engineering Science, Florida State University, Tallahassee, Florida 32306

16. ABSTRACT

A theoretical study and numerical solution are presented for the one-dimensional, time-dependent problem of a streaming, nonuniform, fully ionized, collisionless plasma impinging upon a stationary, flat conducting plate oriented perpendicularly to the flow of the plasma. The problem is intended to model the interaction of the frontal surface of a satellite with the ionospheric plasma.

The time-dependent equations that describe the one-dimensional problem are established, and from them the steady-state equations are derived. These steady-state equations are solved for the spatial dependence of the electric field, which is seen to be a reasonable form and to agree with previous work on more complicated configurations. Finally, a numerical method of solving the time-dependent equations is presented and applied to two special cases: (1) for a plate that has no initial charge, and (2) for a system that is initially in an equilibrium state and proceeds to a second equilibrium state because of a step transition in the plasma parameters.

17. KEY WORDS

Ionosphere
Plasma
Time-Dependent
Satellite
Plasma Sheath

18. DISTRIBUTION STATEMENT

Unclassified - Unlimited

19. SECURITY CLASSIF. (of this report)	20. SECURITY CLASSIF. (of this page)	21. NO. OF PAGES	22. PRICE*
Unclassified	Unclassified	53	$3.00

*For sale by the Clearinghouse for Federal Scientific and Technical Information
Springfield, Virginia 22151

TABLE OF CONTENTS

	Page
SUMMARY	1
INTRODUCTION	1
Purpose	1
Background	1
Approach	2
DERIVATION OF EQUATIONS	3
Time-Dependent Equations	3
Nondimensional Time-Dependent Equations	7
Steady-State Simplification	8
APPLICATION OF NUMERICAL METHODS	9
Modified Euler Method	9
Finite Difference Equations	11
SOLUTION OF CASE I	13
Application of Equations and Boundary Conditions	13
Case I Results	15
SOLUTION OF CASE II	17
Application of Equations and Boundary Conditions	17
Case II Results	18
DISCUSSION	21
Summary	21
Conclusions	21

TABLE OF CONTENTS (Concluded)

Page

APPENDIX A. A PROGRAM FOR THE STEADY-STATE SOLUTIONS 22

APPENDIX B. A PROGRAM FOR THE CASE I TIME-DEPENDENT SOLUTION 25

APPENDIX C. A PROGRAM FOR THE CASE II TIME-DEPENDENT SOLUTION 31

REFERENCES 39

LIST OF ILLUSTRATIONS

Figure	Title	Page
1.	Plasma stream and plate configuration.	6
2.	Spatial distribution of electric potential at 200 km	15
3.	Ion density and velocity distribution in space and time at 200 km.	15
4.	Growth of surface charge on plate at 200 km.	16
5.	Growth of electric potential in space at 200 km	16
6.	Time dependence of the electric field for $\Delta y = 0.1$ and $\Delta T = 0.01$ at 200 km.	16
7.	Time dependence of the electric field for $\Delta y = 0.01$ and $\Delta T = 0.001$ at 200 km.	17
8.	Constant ion density contours at 200 km.	17
9.	Spatial distribution of electric potential at 3000 km	18
10.	Ion density and velocity spatial distribution at 3000 km. . .	19
11.	Effect of increment size on accuracy of spatial distribution.	19
12.	Effect of increment size on accuracy of time dependence	19
13.	Growth of surface charge on plate at 3000 km	20
14.	Growth of electric field at $y = 0.5$ and $y = 1.0$ at 3000 km	20
15.	Growth of electric field at $y = 4.1$ and $y = 5.1$ at 3000 km	20
16.	Growth of electric potential in space for transition from 200- to 3000-km orbit	20

LIST OF TABLES

Table	Title	Page
1.	Ionospheric Parameters	3
2.	Case I Parameters	14
3.	Case II Parameters	18

LIST OF SYMBOLS

English

c	velocity coordinate
e	variable refers to electrons (subscript)
f	velocity distribution function
i	variable refers to ions (subscript)
k	Boltzmann constant
m	mass
n	number density
q	proton charge
t	time coordinate
u	particle velocity
$\bar{u}$	average electron velocity
x	spatial coordinate
y	nondimensional spatial coordinate
D	nondimensional ion number density
E	electric field
F	acceleration caused by body forces
L	Debye length
N	undisturbed number density (electrons or ions)
P	nondimensional electric potential
T	nondimensional time coordinate

LIST OF SYMBOLS (Concluded)

English

T_e	electron temperature
V	nondimensional ion velocity
$\overline{V}$	nondimensional average electron velocity
V_s	satellite velocity
Z	number of charges per ion

Greek

α	ratio of electron and ion kinetic energies
δ	Dirac delta function
ϵ	permittivity
$\hat{E}$	nondimensional electric field
ξ	potential factor
ρ	net charge density
σ	net surface charge density
τ	time factor
ϕ	electric potential
Φ	potential energy

THE ONE-DIMENSIONAL TIME-DEPENDENT INTERACTION OF A SATELLITE WITH THE IONOSPHERIC PLASMA

SUMMARY

The time-dependent equations describing the one-dimensional interaction of a streaming plasma with an infinite flat plate were derived and solved numerically by a modified Euler method. Solutions were obtained for: (1) the case of a plate with no initial surface charge at an altitude of 200 km and (2) the transition from equilibrium conditions at 200 km to an equilibrium state at 3000 km.

In general the surface charge density was found to overshoot to a peak value early in the interaction, as a result of the initial rapid collection of electrons, and slowly decay toward an equilibrium value as the effect of the ions became more pronounced. At 200 km the sheath thickness was found to be 0.33 cm and the relaxation time 1.42 μs, while at 3000 km the sheath thickness and relaxation time were 7.3 cm and 30.5 μs respectively.

INTRODUCTION

Purpose

The net result of the interaction of a body, whether moving or stationary, and a plasma, in which the body is immersed, is a charge accumulation on the surface of the body. The electric potential associated with this charge in turn affects the surrounding plasma, creating a space charge in the disturbed or sheath region near the body.

In this report, a theoretical treatment of the mechanisms that produce the electric potential associated with a body moving through a collisionless ionospheric plasma is undertaken. Special attention is given to the time dependence of the electric field with the intention of investigating the behavior of the various sheath parameters as the body moves rapidly through nonuniform regions of the plasma. A system of equations that describes a one-dimensional model of the problem is established, and numerical methods are invoked to find a solution.

Background

The realm of plasma physics dealing with satellite-ionospheric interactions has grown in interest along with the ever increasing application for and complexity of earth satellites. The sheath effects mentioned above can significantly alter the performance of onboard instrumentation and, therefore, must be taken into account in the planning and interpretation of satellite-borne experiments. Correspondingly, a great volume of work has been done in this area.

To briefly review development in the field, we should first consider an early paper by Jastrow and Pearse in which the effects caused by the motion of a body in a plasma are studied, assuming a spherically symmetrical potential distribution and a uniform, undisturbed ion density [1]. These assumptions have since been found to be incorrect so that the above approach is good only as a first approximation. In a later paper, Kraus and Watson used kinetic equations to calculate the potential and ion number density around a point-like charge moving through the ionosphere [2]. This would imply that the body radius is much smaller than the Debye radius. However, it has been found that the Debye radius in the ionosphere is considerably smaller than the dimensions of a typical satellite. A third paper, published by Davis and Harris and dealing with the same problem, is of interest, because numerical methods were used to solve simultaneously the equations of potential and the motion of ions near a body moving in a plasma [3].

Although these papers provide a good foundation in the area of satellite-ionospheric interactions, none of them attack the time-dependent problem. In fact, in searching the literature for information on the problem treated herein, it was found that relatively little had been done toward the development of a suitable time-dependent theory of the satellite-ionospheric interactions, most of the work having dealt with all aspects of the steady-state interaction for various vehicle geometries.

Some work of a time-dependent nature has been done by G. S. Kino and associates at Stanford

University [4, 5, 6, 7]. However, this work deals with the problem of transmitting rf waves through a discharge plasma and does not apply directly to the problem treated herein. Getmantsev and Denisov have also done work of a time-dependent nature in which they found a plasma disturbance caused by high-frequency electromagnetic field fluctuations near cylindrical bodies slowly moving through a plasma [8]. This work applies only to slowly moving bodies. This is not a good assumption for satellites and, further, would change the nature of the ion interaction since their thermal energy would become important.

Two particular cases of the time-dependent satellite-ionospheric interaction will be treated in detail in this report. First, there is the case in which the satellite has no initial surface charge and is assumed to be at zero potential. Assuming an equal density of ions and electrons in the undisturbed plasma, the more mobile electrons will initially collect on the surface of the satellite at a greater rate than the ions. This will create a negative potential on the satellite that will, in turn, slow the incoming electrons and accelerate the ions, thereby increasing their relative rate of incidence. Hence, as the ion flux at the surface builds, the potential will become more negative at a decreasing rate until an equilibrium condition is reached in which the ion and electron fluxes at the surface of the satellite are equal.

In the second case treated herein the interaction is initially taken to be at some preestablished equilibrium state. A step change is then made in the plasma parameters and the interaction moves to a new equilibrium state.

The general behavior of the interaction in this case is similar to that described previously with the exception that there is an initial surface charge on the satellite and, hence, an electric field that acts on the plasma. The effect of the electric field on the plasma produces the equilibrium state of the previous case. From this point, the electric field increases or decreases to become compatible with the new parameters.

Approach

In order to attack the problem, it was necessary to make several assumptions. First, by taking the body or satellite under consideration to be an infinite flat plate, oriented perpendicularly to the plasma flow, the problem is effectively reduced to one dimension with a corresponding reduction in complexity of the equations. This can be interpreted physically to mean that only a very small region at the stagnation point on the satellite will be considered. Consequently, the electric field, and other sheath parameters, can be observed only in the forward direction. However, the problem is still physically meaningful, since it is conceivable that an infinite flat plate would be a reasonable approximation of a small probe located at the stagnation point of a satellite.

To facilitate the formulation of the problem, we take the inverse of the actual physical situation and let the plasma stream into a stationary plate with the satellite velocity. This will not affect the solution since it is the relative velocity of the satellite, or plate, and the plasma that are important. It should also be noted that any experimental verification in earthbound laboratories will require this arrangement. Since the ion mean thermal velocity in the ionosphere is an order of magnitude less than typical satellite velocities, the random thermal motion of the ions will be neglected. The ions, then, will all have the same velocity at any time and position. The mean thermal velocity of the ionospheric electrons is much greater than typical satellite velocities, and we therefore assume them to have a Maxwellian velocity distribution. Considering the small ratio of electron to ion masses, it is reasonable to assume an instantaneous relaxation of the electrons.

In this treatment we omit the effects of the earth's magnetic field, neutral particle collisions, and corpuscular radiation (photoelectric effect). Since we are dealing with a collisionless plasma in a very small region near the frontal surface of a satellite, these components of the interaction will produce relatively small effects compared with the electric potential resulting from differential charge flux to the surface.

Two further facts about the ionospheric plasma should be brought out before going further into the treatment of the problem. First, as a result of neglecting the ion thermal velocity, we effectively assume zero ion temperature, and therefore only the electrons will be affected by temperature. Any further references to temperature will, therefore, be made to the thermal energy of the electrons. Secondly, the undisturbed, ionospheric plasma is macroscopically neutral so that at any point far from the plate the electron and ion number densities

will be equal. Some feeling for the validity of these and the other assumptions made in this chapter can be obtained by observing the ionospheric parameters. Some typical values are given in Table 1.

In terms of electrical charge, the ionosphere can be considered to be a two-component gas consisting of singly charged ions and electrons. A separate Boltzmann equation must be applied to each species of a multicomponent gas [12]. We will therefore have two equations, one that describes ion velocity distribution and another for electron velocity distribution.

TABLE 1. IONOSPHERIC PARAMETERS

Parameters	Altitude (km)		
	200	300	3000
Satellite Velocity (km/sec)	7.78	7.73	6.52
Ion-Electron Density (m^{-3}) [9]	$(3\text{-}50) \times 10^{10}$	$(10\text{-}20) \times 10^{11}$	7×10^{9}
Temperature (K°) [9]	450-800	1000	4000
Ion-Electron Mean Free Path (m) [9]	90	70	3×10^{4}
Neutral Mean Free Path (m) [9]	80	1000	2×10^{12}
Debye Length (cm) [9]	0.2-1	0.14-0.7	4
Ion Composition [10]	NO^+, O_2^+, O^+	O^+ (98%), N^+	H_e^+
Average Ion Mass	24	16	4
V_s/V_i	13	11	4

DERIVATION OF EQUATIONS

Time-Dependent Equations

The ionospheric plasma must be treated as a collection of discrete particles rather than as a continuous medium. It follows, then, that fluid flow equations used in hydrodynamics and aerodynamics cannot be applied to this type of problem. Nor is it feasible to follow dynamic trajectories of individual particles, except in very limited cases. These difficulties can be circumvented, however, by use of the Boltzmann equation, which provides accurate statistical information about the distribution function and average expected values of quantities describing particle behavior [11]. In its collisionless form, the Boltzmann equation is

$$\frac{\partial f}{\partial t} + c\,\frac{\partial f}{\partial x} + \frac{\partial}{\partial c}\,(fF) = 0 \qquad (1)$$

where f is the distribution function, c is velocity, and F is acceleration resulting from external forces.

As pointed out previously, the electron thermal velocity is much greater than the satellite velocity, and it is therefore reasonable to consider this component of the ionospheric plasma to be at equilibrium. In this case, the electron behavior can be described by the Maxwell-Boltzmann distribution function [13, 14]. In one dimension, this function is of the form,

$$f_e(x,t,c) = N\left(\frac{m_e}{2\pi k T_e}\right)^{1/2} \exp\left[-\frac{m_e c^2}{2kT_e} - \frac{\Phi(x,t)}{kT_e}\right] \qquad (2)$$

where N is the total number of particles in the system, k is the Boltzmann constant, and Φ is the potential energy of the system. This is an exact solution to the steady-state Boltzmann equation. Its use as a time-dependent solution assumes instantaneous relaxation of the electrons.

We now consider the ions. As stated previously, the ion thermal velocity is much smaller than the satellite velocity and can be neglected. The ions will then have a uniform velocity distribution in space and time, which can be written in the form,

$$f_i(x,t,c) = n_i(x,t)\ \delta\left[c + u_i(x,t) \right] \qquad (3)$$

where u_i is the average ion velocity and depends on x and t, and n_i is the ion number density and also depends on x and t.

Multiplying the Boltzmann equation (1) by a constant or any function of ion velocity and integrating over velocity space, we can obtain the equations of transfer, which are more easily solved than the Boltzmann equation [15]. Using the ion mass, m_i, as the multiplier and performing the appropriate integration, we obtain

$$\int_{-\infty}^{0} m_i \left[\frac{\partial f_i}{\partial t} + c\,\frac{\partial f_i}{\partial x} + \frac{\partial}{\partial c}\,(F f_i) \right] dc = 0$$

or

$$\int_{-\infty}^{0} \frac{\partial f_i}{\partial t}\,dc + \int_{-\infty}^{0} c\,\frac{\partial f_i}{\partial x}\,dc + \int_{-\infty}^{0} \frac{\partial}{\partial c}\,(F f_i)\,dc = 0 \ .$$

Since x and t are independent variables, the partial derivatives of these variables can be brought outside the integral. Performing this operation and replacing f_i by expression (3), we obtain

$$\frac{\partial}{\partial t}\left[n_i \int_{-\infty}^{0} \delta(c + u_i)\,dc \right]$$

$$+ \frac{\partial}{\partial x}\left[n_i \int_{-\infty}^{0} c\,\delta(c + u_i)\,dc \right]$$

$$+ F n_i \int_{-\infty}^{0} \frac{\partial}{\partial c}\left[\delta(c + u_i) \right] dc = 0 \ .$$

Notice that the third term reduces to $F n_i \delta(c-u_i)\,|_{-\infty}^{0}$, which is zero at both limits. The remaining terms have values only when $c = -u_i$. The foregoing expression therefore reduces to

$$\frac{\partial}{\partial t}\,(n_i) + \frac{\partial}{\partial x}\left[n_i(-u_i) \right] = 0$$

or

$$\frac{\partial}{\partial t}\left[n_i(x,t) \right] - \frac{\partial}{\partial x}\left[n_i(x,t)\ u_i(x,t) \right] = 0 \ . \qquad (4)$$

This is the conservation of mass, or continuity equation for ions.

By multiplying the Boltzmann equation (1) by $1/2\ m_i c^2$ and integrating over velocity space in a similar manner, we can obtain the conservation of energy equation for ions. The integration is carried out as follows:

$$\int_{-\infty}^{0} \frac{1}{2}\,m_i c^2 \left[\frac{\partial f_i}{\partial t} + c\,\frac{\partial f_i}{\partial x} + \frac{\partial}{\partial c}\,(F f_i) \right] dc = 0$$

$$\frac{\partial}{\partial t}\left[n_i \int_{-\infty}^{0} c^2\,\delta(c + u_i)\,dc \right]$$

$$+ \frac{\partial}{\partial x}\left[n_i \int_{-\infty}^{0} c^3\,\delta(c - u_i)\,dc \right]$$

$$+ F n_i \int_{-\infty}^{0} c^2\,\frac{\partial}{\partial c}\left[\delta(c + u_i) \right] dc = 0 \ .$$

The acceleration, F, results from the electric field associated with the plate and is therefore qE/m_i, where E is a function of x and t. The acceleration, F, can therefore be taken out of the integral since in this case it is not a function of velocity. This yields

$$\frac{\partial}{\partial t}\left[n_i(-u_i)^2\right] + \frac{\partial}{\partial x}\left[n_i(-u_i)^3\right] + Fn_i\left\{\left[c^2\,\delta(c+u_i)\right]_{-\infty}^{0} - \int_{-\infty}^{0} 2c\,\delta(c+u_i)\,dc\right\} = 0 \quad .$$

Note that the term $c^2\delta(c - u_i)\,|_{-\infty}^{0}$ is zero at both limits, and the integral is $2(-u_i)$. The preceding expression now simplifies to the form,

$$\frac{\partial}{\partial t}\left[n_i(x,t)\,u_i^2(x,t)\right] - \frac{\partial}{\partial x}\left[n_i(x,t)\,u_i^3(x,t)\right] + \frac{2q}{m_i}\,E(x,t)\,n_i(x,t)\,u_i(x,t) = 0 \quad ,$$

where we have replaced F by qE/m_i. This equation can be simplified if we first expand the terms to obtain

$$2n_i u_i \frac{\partial}{\partial t}(u_i) + u_i^2 \frac{\partial}{\partial t}(n_i) - n_i u_i \frac{\partial}{\partial x}(u_i^2) - u_i^2 \frac{\partial}{\partial x}(n_i u_i) + \frac{2q}{m_i} En_i u_i = 0 \quad .$$

Rearranging terms we get

$$2n_i u_i \frac{\partial}{\partial t}(u_i) + u_i^2\left[\frac{\partial}{\partial t}(n_i) - \frac{\partial}{\partial x}(n_i u_i)\right] - 2n_i u_i^2 \frac{\partial}{\partial x}(u_i) + \frac{2q}{m_i} En_i u_i = 0 \quad .$$

Now the term in brackets is exactly equation (4), which is equal to zero. We can also divide the remaining terms by $2n_i u_i$ to obtain

$$\frac{\partial}{\partial t}\left[u_i(x,t)\right] - u_i(x,t)\frac{\partial}{\partial x}\left[u_i(x,t)\right] + \frac{q}{m_i}E(x,t) = 0 \quad , \qquad (5)$$

which is the conservation of energy equation for ions.

In the above derivations, the limits of integration are taken from $-\infty$ to 0, because the ions move in the negative x-direction when traveling toward the plate. The 0 to $+\infty$ range is not included because all ions that strike the conducting plate are absorbed or neutralized. Since all ions initially stream toward the plate and none are reflected, there can be no positive component of the ion velocity distribution (Fig. 1).

The two foregoing conservation equations contain the three dependent variables, n_i, u_i, and E. A third equation is, therefore, required to obtain a solution. This is provided by Gauss' equation, which in its general form is

$$\nabla \cdot \vec{E}(x,t) = \rho(x,t)/\epsilon_0 \quad . \qquad (6)$$

In the above equation ρ is the net charge density per unit volume. Note that we have not used the wave equation because the potential retardation term, $1/c^2\,(\partial^2\phi/\partial t^2)$, is assumed to be negligible for this case.

The net charge density is obtained by adding the total charge density of ions and electrons as follows:

$$\rho(x,t) = q\left[Zn_i(x,t) - n_e(x,t)\right] \quad . \qquad (7)$$

Here, Z represents the number of charges per ion. However, since we assume only singly ionized particles to exist, Z will have a value of unity. The number densities, n_i and n_e, are average values. The ion average number density, n_i, must be obtained from the solution of the equations; however, the electron average number density can be found from expression (2) as follows [16]:

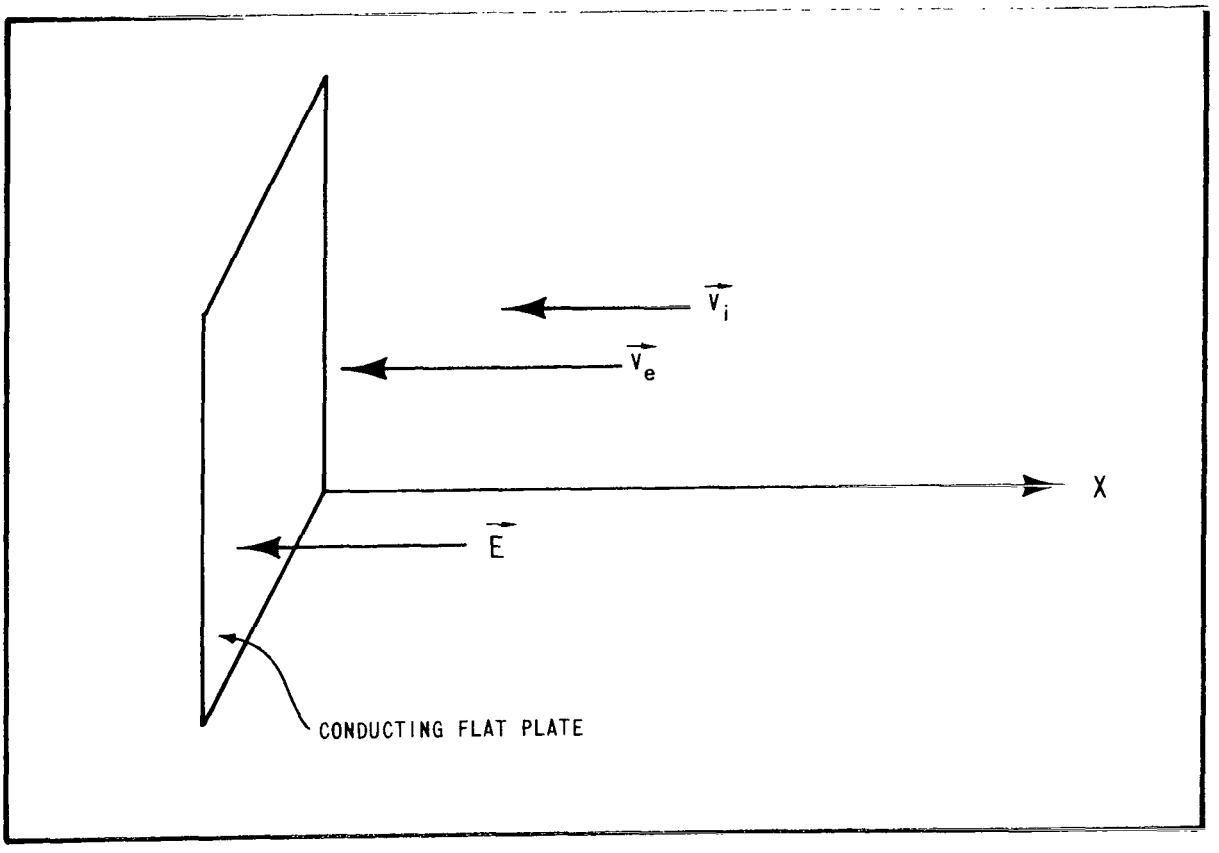

Figure 1. Plasma stream and plate configuration.

$$n_e = \int_{-\infty}^{\infty} f_e \, dc$$

$$= \int_{-\infty}^{\infty} N \left(\frac{m_e}{2\pi kT_e}\right)^{1/2} e^{-\left[\left(\frac{m_e}{2kT_e}\right)c^2 \quad \Phi/kT_e\right]} dc$$

$$= N \left(\frac{m_e}{2\pi kT_e}\right)^{1/2} e^{-\Phi/kT_e} \int_{-\infty}^{\infty} e^{-\left(\frac{m_e}{2kT_e}\right)c^2} dc$$

$$= N \left(\frac{m_e}{2\pi kT_e}\right)^{1/2} e^{-\Phi/kT_e} \left(\frac{2\pi kT_e}{m_e}\right)^{1/2}$$

$$n_e = N e^{-\Phi/kT_e} \quad .$$

The potential energy for electrons, Φ, is equal to $-q\phi$ where ϕ is the electric potential. This can, in turn, be written in terms of the electric field as follows:

$$\vec{E} = -\nabla\phi = -d\phi/dx \, \hat{i}$$

$$\int_x^{\infty} E \, dx = -\int_{\phi}^{0} d\phi' = \phi \quad .$$

Then the electron number density can be written in the form

$$n_e(x,t) = N e^{\frac{q}{kT_e} \int_{x'}^{\infty} E(x,t) \, dx} \qquad (8)$$

Substituting equation (8) and equation (7) into equation (6), we obtain Poisson's equation in the form

$$\frac{\partial E(x,t)}{\partial x} = \frac{q}{\epsilon_0}\left[n_i(x,t) - N\, e^{\frac{q}{kT_e}\int_{x'}^{\infty} E(x,t)\,dx}\right] . \quad (9)$$

The boundary conditions for the system of equations (4), (5), and (9) can be described in terms of the electric field, which must go to zero for any set of initial conditions and time as the distance from the plate approaches infinity. At the plate, the value of the electric field will depend upon the initial conditions. However, its change with time can always be represented by the difference of the ion and electron fluxes to the plate. Therefore,

$$\frac{\partial \sigma}{\partial t} = q(n_i u_i - n_e u_e)\Big|_{x\,=\,0}$$

The average values, n_e and u_e, can be represented as follows:

$$n_e = N\, e^{\frac{q}{kT_e}\int_0^{\infty} E\,dx} .$$

This was shown previously in equation (8). Similarly,

$$u_e = \int_{-\infty}^{\infty} \frac{c}{N} f_e\, dc = \bar{u}\, e^{\frac{q}{kT_e}\int_0^{\infty} E\,dx}$$

where

$$\bar{u} = (kT_e/2\pi m_e)^{1/2} .$$

Now, from Gauss' Law it can be shown that $E = \sigma/\epsilon_0$ [17]. Applying this and the two expressions for n_e and u_e found previously, we obtain

$$\frac{\partial E(0,t)}{\partial t} = \frac{q}{\epsilon}\left[n_i(0,t)\, u_i(0,t) - N\bar{u}\, e^{\frac{2q}{kT_e}\int_0^{\infty} E(x,t)\,dx}\right] \quad (10)$$

which is the desired boundary condition.

The set of initial conditions will depend on the particular case being solved and will therefore be given later in the report rather than here.

Nondimensional Time-Dependent Equations

The set of equations derived in the previous section will be more manageable in the numerical analysis if they are nondimensionalized. We define nondimensional density, $D = n_i/N$; velocity, $V = u_i/V_s$; distance from the plate, $y = x/L$; time, $T = t/\tau$, and electric field $\hat{E} = E/\xi$, where N is the undisturbed ion number density, V_s is the satellite velocity, and L, τ, and ξ must be determined. In terms of these variables, equation (4) takes the form

$$\frac{\partial D}{\partial T} - \frac{\tau V_s}{L}\frac{\partial}{\partial y}(DV) = 0 .$$

Now if we let $\tau = L/V_s$, then the previous equation becomes

$$\frac{\partial D(y,T)}{\partial t} - D(y,T)\frac{\partial V(y,T)}{\partial y} - V(y,T)\frac{\partial D(y,T)}{\partial y} = 0 , \quad (11)$$

which is the nondimensional continuity equation.

Now consider equation (5). Upon substitution of the nondimensional variables, it takes the form

$$\frac{V_s}{\tau}\frac{\partial V}{\partial T} - \frac{V_s^2}{L}\frac{\partial V}{\partial y} + \frac{q\xi}{m_i}\hat{E} = 0 .$$

Now recall that τ has been defined as L/V_s. Making this substitution leads to the form,

$$\frac{\partial V}{\partial T} - V\frac{\partial V}{\partial y} + \left(\frac{q\xi L}{m_i V_s^2}\right)\hat{E} = 0 .$$

By defining $\alpha = (q\xi L)/(m_i V_s^2)$ where α determines the amount of effect the electric field has on ion velocity, we obtain the following nondimensional form of the energy conservation equation:

$$\frac{\partial V(y,T)}{\partial T} - V(y,T)\,\frac{\partial V(y,T)}{\partial y} + \alpha\,\hat{E}(y,T) = 0 \quad . \tag{12}$$

Similarly, equation (9) takes the following form:

$$\frac{\partial \hat{E}}{\partial y} = \frac{q\,NL}{\xi\epsilon_0}\left[D - e^{\frac{q\xi L}{kT_e}\int_{y'}^{\infty}\hat{E}\,dy} \right] .$$

The exponent must be dimensionless, so we define $\xi = kT_e/qL$. Substituting this definition of ξ into the coefficient of the term on the right side of the equation yields $q^2NL^2/(\epsilon_0 kT_e)$. This can be made dimensionless by defining $L = \sqrt{\epsilon_0 kT_e/q^2n}$. The above equation now becomes

$$\frac{\partial \hat{E}(y,T)}{\partial y} = D(y,T) - e^{\int_{y'}^{\infty}\hat{E}(y,T)\,dy} \quad , \tag{13}$$

which is the nondimensional Poisson's equation.

Finally, equation (10) must be nondimensionalized. Making the variable substitutions, it takes the following form:

$$\frac{\partial \hat{E}}{\partial T} = \frac{q\tau\,N\,V_s}{\epsilon_0\,\xi}\left[DV - \bar{u}/V_s\; e^{2\int_0^{\infty}\hat{E}\,dy} \right] .$$

Recall now that $\tau = L/V_s$ so that the coefficient of the term on the right side of the equation becomes $(qNL/\epsilon_0)/\xi$, which is unity since $\xi = kT_e/qL$ and $L = \sqrt{\epsilon_0\,kT_e/q^2N}$. Now if we let $\bar{V} = \bar{u}/V_s$, the above equation becomes

$$\frac{\partial \hat{E}(y,T)}{\partial T} = D(y,T)\,V(y,T) - \bar{V}\,e^{2\int_0^{\infty}\hat{E}(y,T)\,dy'} \quad , \tag{14}$$

which is the nondimensional form of the boundary condition at the plate.

The factors L, τ, and ξ have all been defined. Now each can be expressed in terms of the plasma parameters. We already have $L = \sqrt{\epsilon_0\,kT_e/q^2N}$. Using this expression for L in the expression for τ, we obtain $\tau = \sqrt{\epsilon_0\,kT_e/q^2NV_s^2}$. Similarly, $\xi = \sqrt{NkT_e/\epsilon_0}$ and $\alpha = kT_e/m_iV_s^2$.

Steady-State Simplification

The equations describing the steady-state interaction can be derived directly from the time-dependent equations (11), (12), (13), and (14) be setting all derivatives with respect to time equal to zero. Thus equation (11) becomes

$$\frac{d}{dy}\left[D(y,T)\,V(y,T) \right] = 0 \quad . \tag{15}$$

By dropping the time derivative in equation (12) we get

$$\alpha\,\hat{E} = V\,\frac{dV}{dy} \quad .$$

Integrating both sides of this equation with respect to y we obtain

$$\int_y^{\infty}\hat{E}\,dy = \frac{1}{\alpha}\int_V^1 V'\,dV'$$

or

$$P(y) = \frac{1}{2\alpha}\left[V^2(y) - 1 \right] \tag{16}$$

where P denotes the nondimensional electric potential.

Equation (13) takes the form

$$\frac{d\hat{E}}{dy} = D - e^{\int_y^\infty \hat{E}\, dy} ,$$

or in terms of the nondimensional, electric potential, P, it is

$$\frac{d^2P(y)}{dy^2} = e^{P(y)} - D(y) . \qquad (17)$$

Equations (15), (16), and (17) can now be combined into a single equation for the electric potential. Notice that equation (15) implies that DV = constant. This constant is required to be unity by the boundary conditions on ion density and velocity at infinity. Then we obtain the solution

$$D(y) = 1/V(y) . \qquad (18)$$

Equation (16) can be solved for V(y) to obtain $\sqrt{1-2\alpha P}$. Replacing V in equation (18) with this expression we obtain

$$D = 1/\sqrt{1-2\alpha P} .$$

This expression can, in turn, be used to replace D in equation (17) to obtain

$$\frac{d^2P(y)}{dy^2} = e^{P(y)} - \frac{1}{\sqrt{1-2\alpha P(y)}} , \qquad (19)$$

which provides an equation of P as a function of y and the plasma parameters.

The boundary condition at the plate given by equation (14) can also be used in the steady-state solution. Equating $\partial\hat{E}/\partial t$ to zero, we obtain

$$DV - \overline{V}\, e^{2\int_0^\infty \hat{E}\, dy} = 0 .$$

The integral of the electric field, in this equation, is just the electric potential at the origin, or plate, which will be designated as P_0. Making this substitution and solving for P_0 we find that

$$P_0 = \frac{1}{2} \ln (DV/\overline{V}) , \qquad (20)$$

which is the potential on the plate for a given set of plasma parameters.

The solution of equations (16), (17), (18), (19), and (20) by numerical methods is simpler and less subject to error than a numerical solution of the time-dependent equations of the previous section. Their solution will therefore provide a check on the degree of approach to the steady-state solution of the time-dependent equations.

APPLICATION OF NUMERICAL METHODS

Modified Euler Method

Given a differential equation and its solution at some initial or boundary point, the solution can be extrapolated to a neighboring point by use of the Taylor series. This is an infinite series of the form

$$Y_{n+1} = Y_n + M_n h + \frac{1}{2} M'_n h^2 + \frac{1}{6} M''_n h^3 + \ldots \qquad (21)$$

where $M_n = (dY/dx)_n$, $M'_n = (d^2Y/dx^2)_n, \ldots$, all of which are evaluated at the point $x_n = x_0 + nh$, where $h = x_{n-1} - x_n$. Although this method is accurate if h is sufficiently small, it is not frequently used in this form since it usually requires more work than other methods. It is useful, however, in finding the first few points of a solution, which, as will be seen, cannot always be obtained from other methods.

The method used herein is a modification of the Euler method. To describe it, we begin first with the Euler method itself, which is the oldest and most straightforward method of analysis, but is also relatively crude and inaccurate.

If the increment, h, in the Taylor series (21) is taken to be much less than unity, the first two terms will provide reasonably good accuracy. The solution at the neighboring point then becomes

$$Y_{n+1} = Y_n + M_n h \quad . \tag{22}$$

The solution is expanded to increasingly remote points from the initial point by the process

$$Y_{n+2} = Y_{n+1} + M_{n+1} h \quad ,$$

$$Y_{n+3} = Y_{n+2} + M_{n+2} h \quad , \quad \text{etc.}$$

This process is known as the Euler method.

While the first few points can be made sufficiently accurate by picking h small enough, as the solution progresses, the error will become increasingly larger. This occurs because the differential, M_n, (the slope of the solution curve at x_n) is used to calculate the solution Y_{n+1} at x_{n+1}. The calculation of Y_{n+1} will therefore be in error by an amount equal to the difference in the slopes at x_{n+1} and x_n, multiplied by the increment. Further the total error in the solution Y_{n+1} is the sum of the error in calculating Y_{n+1} and the errors in calculating all previous solutions. The fallacy in this method is discussed very well by Scarborough [18].

By using the modified Euler method, the cumulative error in the previous method is avoided. Here an average value of the differential is used in calculating each succeeding point. The extrapolated solution Y_{n+1} is therefore of the form

$$Y_{n+1} = Y_n + \frac{1}{2}\left(M_n + M_{n+1}\right) h \tag{23}$$

where M_n is the derivative of Y at x_n and M_{n+1} is the derivative of Y at x_{n+1}. This method requires the use of a less accurate solution of Y_{n+1} such as equation (22), which is inserted into the differential equation in order to find the value of M_{n+1}. This value is, in turn, used to calculate a new and more accurate value of Y_{n+1} from equation (23). The process can be repeated, using the new value for Y_{n+1}, until the desired accuracy is attained [19].

The trouble with the above method lies in the need to determine the derivatives of each variable involved. For the complex set of equations derived in the DERIVATION OF EQUATIONS section of this report, this is no easy matter. However, the same general averaging effect can be obtained in the following way, which, although less accurate, is more straightforward and easier to apply to the problem at hand.

First, we observe that the solution Y_{n-1} can be obtained by replacing h by -h wherever it appears in equation (21). Subtracting the resulting equation from equation (21), we obtain

$$Y_{n+1} = Y_{n-1} + 2M_n h + \frac{2}{6} M_n'' h^3 + \ldots$$

If h is again taken to be less than unity and terms of order h^3 and higher are dropped, we obtain

$$Y_{n+1} = Y_{n-1} + 2M_n h \quad . \tag{24}$$

The accuracy of this formulation is much improved over that of the unmodified Euler method shown in equation (22). This is evident by the fact that the Euler method neglects all terms in the Taylor series of order h^2 or higher, whereas this method only drops terms of h^3 or higher.

The extension of the above method to partial differential equations is rather straightforward, although stability is a much greater problem here, and some care must be exercised to ensure that the solution behaves in a stable manner [20].

The partial derivative of Y with respect to x at x_n and t_k has the form

$$\left(\frac{\partial Y}{\partial x}\right)_n = \frac{Y_{n+1,k} - Y_{n-1,k}}{2\Delta x} \quad , \tag{25}$$

which is of the same form as equation (24). It would at first appear that the time derivative of Y could be written in the same form. However, this would require the storage of three arrays in the computer. Instead, the following form has proven to be more useful:

$$\left(\frac{\partial Y}{\partial t}\right)_n = \frac{Y_{n,k+1} - \frac{1}{2}\, Y_{n+1,k} + Y_{n-1,k}}{\Delta t} \quad . \tag{26}$$

Here, the second value in the finite difference has been averaged over two increments within the same time frame. This formulation will be stable provided we choose Δt according to the relation

$$\Delta t \leq \Delta x/u \tag{27}$$

where u is the characteristic velocity involved. This is equivalent to requiring Δt to be smaller than the time required for a quantity to cross the Δx grid [21].

For the solution at a boundary where $n = 0$ and, therefore, the subscript $(n-1)$ has no meaning, we require the less accurate forms,

$$\left(\frac{\partial Y}{\partial t}\right)_n = \frac{Y_{n,k+1} - Y_{n,k}}{\Delta t} \tag{28}$$

and

$$\left(\frac{\partial Y}{\partial x}\right)_n = \frac{Y_{n+1,k} - Y_{n,k}}{\Delta x} \quad , \tag{29}$$

which are based on the unmodified Euler method and will, in general, be used only for the first two terms of the solution.

Finite Difference Equations

The numerical equations can now be formulated by applying the appropriate relations in the foregoing section to the equations developed in the DERIVATION OF EQUATIONS section. Before going on, however, it should be pointed out, as in the Modified Euler Method section and as is apparent from equation (25), that the modified Euler method cannot be used to find the first two points of the solution. Two sets of difference formulas will, therefore, be required for any given equation. The first set will be based upon the relations (28) and (29) and will be used to find only the first two points in x for each time frame. The solution at all other points will be found from the second set of equations, which will be based on relations (25) and (26).

First, consider the steady-state equations given in the Steady-State Simplification section. The form of the potential is given by equation (19) which we repeat below:

$$\frac{d^2P(y)}{dy^2} = e^{P(y)} - \frac{1}{\sqrt{1 - 2\alpha P(y)}} \quad . \tag{19}$$

For this equation, the accuracy of the unmodified Euler method given in equation (22) was found to be sufficient. An extension of equation (22) to the second derivative yields

$$\frac{d^2y}{dx^2} = \frac{Y_{n+1} - 2Y_n + Y_{n-1}}{\Delta x^2} \quad . \tag{30}$$

Applying equation (30) to equation (19) we find

$$\frac{P_{n+1} - 2P_n + P_{n-1}}{\Delta y^2} = e^{P_n} - 1\sqrt{1 - 2\alpha P_n} \quad .$$

solving for P_{n+1} we obtain

$$P_{n+1} = 2P_n - P_{n-1} + \Delta y^2 e^{P_n} - \Delta y^2/\sqrt{1 - 2\alpha P_n}, \tag{31}$$

which will provide a solution for the potential at all spatial points, with the exception of the first two at the origin. The ion velocity can be found from equation (16):

$$P(y) = \frac{1}{2\alpha}\left[V^2(y) - 1\right] \quad . \tag{16}$$

Solving this equation for V and writing the variables as functions of y_n, we obtain,

$$V_n = \sqrt{1 - 2\alpha P_n} \quad . \tag{32}$$

From equation (18) we have the following relation for density:

$$D_n(y) = 1/V_n(y) \tag{33}$$

Finally, the steady-state potential on the plate, needed to give the solution the correct magnitude, can be found from equation (20), which written as a function of y, is of the form

$$P_0 = \frac{1}{2} \ln (D_0 V_0/\overline{V}) \quad . \tag{34}$$

The equations (31), (32), (33), and (34) can now be programmed for a numerical solution to the steady-state case. This program is given in Appendix A.

We consider now the time-dependent equations given in the Nondimensional Time-Dependent Equations section of this report. For convenience we repeat equations (11), (12), (13), and (14) below:

$$\frac{\partial D(y,T)}{\partial t} - D(y,T)\frac{\partial V(y,T)}{\partial y} - V(y,T)\frac{\partial D(y,T)}{\partial y} = 0 \tag{11}$$

$$\frac{\partial V(y,T)}{\partial t} - V(y,T)\frac{\partial V(y,T)}{\partial y} + \alpha \hat{E}(y,T) = 0 \tag{12}$$

$$\frac{\partial \hat{E}(y,T)}{\partial y} = D(y,T) - e^{\int_{y'}^{\infty} \hat{E}(y,T)\,dy} \tag{13}$$

$$\frac{\partial \hat{E}(0,T)}{\partial T} = D(y,T)\,V(y,T) - \overline{V}\, e^{2\int_{0}^{\infty} \hat{E}(y,T)\,dy} \tag{14}$$

Expressing these equations in the difference forms of equations (28) and (29) we obtain

$$\frac{D_{n,k+1} - D_{n,k}}{\Delta T} - D_{n,k}\left(\frac{V_{n+1,k} - V_{n,k}}{\Delta y}\right) - V_{n,k}\left(\frac{D_{n+1,k} - D_{n,k}}{\Delta y}\right) = 0 \tag{35}$$

$$\frac{V_{n,k+1} - V_{n,k}}{\Delta T} - V_n\left(\frac{V_{n+1,k} - V_{n,k}}{\Delta y}\right) + \alpha \hat{E}_{n,k} = 0 \tag{36}$$

$$\frac{\hat{E}_{n+1,k} - \hat{E}_{n,k}}{\Delta y} = D_{n,k} - e^{\sum_{n=y}^{\infty}{}' \hat{E}_{n,k}\Delta y} \tag{37}$$

and

$$\frac{\hat{E}_{n,k+1} - \hat{E}_{n,k}}{\Delta T} = D_{n,k}V_{n,k} - \overline{V}\, e^{2\sum_{n=y}^{\infty}{}' \hat{E}_{n,k}\Delta y} \tag{38}$$

Solving equations (35), (36), (37), and (38) for the appropriate variables, we find the following set of equations:

$$D_{n,k+1} = D_{n,k} + \left[D_{n,k}\left(\frac{V_{n+1,k} - V_{n,k}}{\Delta y}\right) + V_{n,k}\left(\frac{D_{n+1,k} - D_{n,k}}{\Delta y}\right)\right]\Delta T \tag{39}$$

$$V_{n,k+1} = V_{n,k} + V_{n,k}\left(\frac{V_{n+1,k} - V_{n,k}}{\Delta y}\right)\Delta T - \alpha \hat{E}_{n,k}\Delta T \tag{40}$$

$$\hat{E}_{n+1,k} = \hat{E}_{n,k} + \left(D_{n,k} - e^{\sum_{n=y}^{\infty}{}' \hat{E}_{n,k}\Delta y}\right)\Delta y \tag{41}$$

$$\hat{E}_{0,k+1} = \hat{E}_{0,k} + \left(D_{0,k} V_{0,k} - \overline{V}\, e^{2\sum_{n=0}^{\infty} \hat{E}_{n,k} \Delta y} \right) \Delta T \quad . \tag{42}$$

The above set of equations is used to obtain solutions to the variables at the plate boundary in all time frames.

By applying the difference formulations in equations (25) and (26) to equations (11), (12), and (13), we obtain

$$\frac{D_{n,k+1} - \overline{D_{n,k}}}{\Delta T} - D_{n,k} \left(\frac{V_{n+1,k} - V_{n-1,k}}{2\Delta y} \right) - V_{n,k} \left(\frac{D_{n+1,k} - D_{n-1,k}}{2\Delta y} \right) = 0 \tag{43}$$

$$\frac{V_{n,k+1} - \overline{V_{n,k}}}{\Delta T} - V_{n,k} \left(\frac{V_{n+1,k} - V_{n-1,k}}{2\Delta y} \right) + \alpha \hat{E}_{n,k} = 0 \tag{44}$$

$$\frac{\hat{E}_{n+1,k} - \hat{E}_{n-1,k}}{2\Delta y} = D_{n,k} - e^{\sum_{n=y}^{\infty} \hat{E}_{n,k} \Delta y} \tag{45}$$

where any quantity $\overline{W_{n,k}}$ is defined as $1/2 \left(W_{n+1,k} + W_{n-1,k} \right)$. Solving these equations for the appropriate variable we obtain the following:

$$D_{n,k+1} = \frac{1}{2} \left(D_{n+1,k} + D_{n-1,k} \right) + \left[D_{n,k} \left(\frac{V_{n+1,k} - V_{n-1,k}}{2\Delta y} \right) + V_{n,k} \left(\frac{D_{n+1,k} - D_{n-1,k}}{2\Delta y} \right) \right] \Delta T \tag{46}$$

$$V_{n,k+1} = \frac{1}{2} \left(V_{n+1,k} + V_{n-1,k} \right) + V_{n,k} \left(\frac{V_{n+1,k} - V_{n-1,k}}{2\Delta y} \right) \Delta T - \alpha \hat{E}_{n,k} \Delta T \tag{47}$$

$$\hat{E}_{n+1,k} = \hat{E}_{n-1,k} + \left(D_{n,k} - e^{\sum_{n=y}^{\infty} \hat{E}_{n,k} \Delta y} \right) 2\Delta y \quad . \tag{48}$$

This set of equations can be used in any time frame to find a solution to the problem at all points in space with the exception of those points on the plate.

The above sets of equations, (39), (40), (41), and (42) and (46), (47), and (48), can now be programmed for a numerical solution of the time-dependent problem. This program is included in Appendix B.

SOLUTION OF CASE I

Application of Equations and Boundary Conditions

In this first case to be treated it is assumed that the conducting plate initially has no electric potential. The plate is then allowed to float, its potential being determined by the ratio of the impinging ion and electron fluxes. The physical parameters governing this particular case are listed in Table 2. The boundary conditions imposed on the equations for this case are as follows:

a. Initially, the parameters of the undisturbed plasma will apply at all points in space. On this basis, the electric field is zero everywhere while the nondimensional ion density and velocity are both unity.

b. The ion density and velocity must at any time go to their undisturbed values (unity) and the electric field to zero at very large distances from the plate.

c. The electric potential on the plate is given by the relation in equation (34) for the steady-state equations, and the electric field at the plate is given

TABLE 2. CASE I PARAMETERS

Symbol	Parameter	Value
-	Altitude[a] (km)	200
N	Ion-Electron Density[a] (m^{-3})	$(3\text{-}50) \times 10^{10}$
T_e	Temperature[a] (K°)	450-800
m_i	Average Ion Mass[a] (Amu)	24
$\bar{u}$	Average Electron Velocity[b] (km/sec)	43.928
V_s	Satellite Velocity[a] (km/sec)	7.780
L	Debye Length[b] (cm)	0.276
ξ	Potential Factor[b] (volt/m)	24.973
τ	Time Factor[b] (sec)	0.3548×10^{-6}

a. From Table 1
b. Calculated Values

at any time by equation (42) for the time-dependent equations.

To determine the other parameters, such as nondimensional electron velocity, Debye length, etc., we must refer to specific values of the plasma parameters given in Table 1. With this information, the values of the nondimensional average electron velocity ($\bar{V}$), Debye length (L), characteristic time (τ), nondimensional potential factor (ξ), and a factor that determines the effectiveness of the electric body force on the ions (α), can be determined from relations given in the Nondimensional Time-Dependent Equations section. These values are given in Table 2 along with the data from which they were calculated.

The steady-state program (Appendix A) is relatively simple, and, in principle, it can be made as accurate as desired by properly choosing the increment size, allowable error, and the magnitude of the assumed potential. Accuracy of more than four significant figures is unnecessary here, however, since the general behavior is important and higher accuracy would not visibly alter plots of the data. This is the more accurate of the two programs and should certainly be considered to give more reliable steady-state values.

The program for the time-dependent solution (Appendix B) is considerably more complex, and an analysis of its accuracy is not so straighforward. Since it solves the partial differential equations, it has finite differences in both time and position. As a result, the error, which would normally be associated with a finite difference treatment of ordinary differential equations of one variable, is compounded by the second difference relation. This is further complicated by the restriction equation (27) places on the ratio of the increments of the two independent variables in order to attain a stable solution. This ratio was found to be extremely critical. It should also be noted that, because finite differences are used, the solution consists of small step-like increments rather than a continuous curve. The consequence of this can best be seen by taking the electric field as an example. Once the zero boundary condition far from the plate has been approached to within a critical value, the next solution step, rather than going smoothly to zero, crosses over into the positive region. Zero is missed because it is located only a fraction of an increment from the last step in the solution. However, once the electric field becomes positive, the solution becomes unstable and grows at an increasing rate.

The above effect is strictly a result of using finite difference approximations and has no physical foundation. However, to prevent its occurrence, it was necessary to force the electric field to go to zero whenever this situation took place. While this may seem arbitrary, it can be argued that this truncation does not affect the solution appreciably since the field is very close to zero whenever the instability occurs.

Case I Results

In the discussion to follow, the term steady-state will refer to the solution of the steady-state equations of the Steady-State Simplification section, while the solution of the time-dependent equations of the Nondimensional Time-Dependent Equations section will be described as asymptotically approaching equilibrium (hereafter referred to as quasi-equilibrium).

The plots of the quasi-equilibrium and steady-state electric potential given in Figure 2 are seen to be in very good agreement. The data points given in this figure are the results of the numerical solution of steady-state equations (31), (32), (33), and (34) where the curves result from the numerical, quasi-equilibrium solution of time-dependent equations (39), (40), (41), (42), (46), (47), and (48). The quasi-equilibrium values occur at $t = 1.42\ \mu s$ and we use the standard definition P_0/e for sheath thickness. Hence, the quasi-equilibrium sheath thickness at 200 km is found to be 0.33 cm.

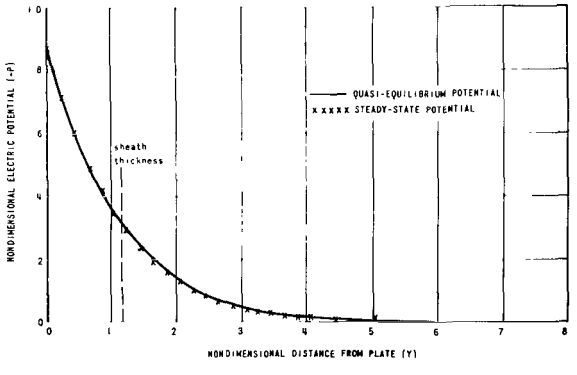

Figure 2. Spatial distribution of electric potential at 200 km.

The response of the ions to the electric field can be seen in Figure 3, which shows the development in time of both the ion velocity and density, along with the steady-state solution. At $t = 1.42\ \mu s$, the time dependent solutions (denoted by curves) have essentially reached their equilibrium values, and the discrepancy between the quasi-equilibrium curve and the steady-state solution (shown as data points) is attributable to round-off error and the relatively large increment size used. This will be discussed in more detail at the end of this section.

From the steady-state continuity equation we have the requirement DV = 1 everywhere in space.

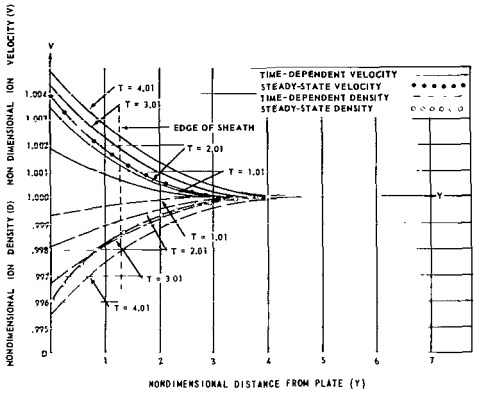

Figure 3. Ion density and velocity distribution in space and time at 200 km.

Therefore, as a check on the accuracy of the numerical solutions, the quasi-equilibrium flux and steady-state flux at the plate ($y = 0$) and at the edge of the sheath ($y = 1.2$) were compared with unity. The quasi-equilibrium and steady-state flux differed from unity by 0.000579 and 0.0000152 at $y = 0$ and 0.000505 and 0.0000520 at $y = 1.2$ respectively, thus showing the solutions to have good accuracy, with the steady-state solution being slightly better as expected.

The growth of electric charge on the plate, given in Figure 4, indicates the charge behavior relatively early in the interaction, which primarily is due to electrons at this point. Initially, all electrons impinge on the plate and deposit charge there, but as the plate potential becomes more negative, increasing numbers of electrons are repelled and the rate of charge deposition decreases. The influence of the ions cannot be seen in the early stages of the interaction shown here. However,

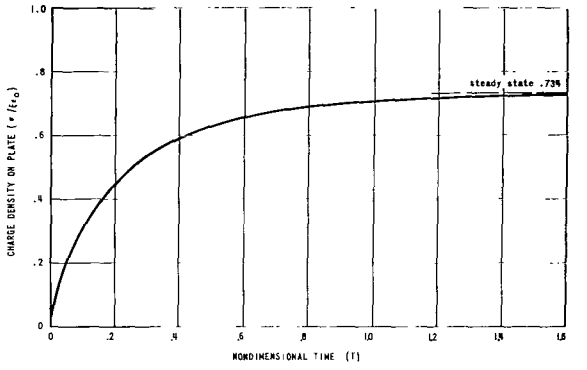

Figure 4. Growth of surface charge on plate at 200 km.

they have a very pronounced effect that takes place much later, which will be discussed in the following chapter.

Figure 5 shows the development of the electric potential in time and space and illustrates very well the approach of the solution to an equilibrium value.

An instability that occurred very early in the numerical solution of the time-dependent electric field is shown in Figures 6 and 7. This effect is strictly the result of error in the numerical calculations as is indicated by the difference in the two curves affected by changing increment sizes. Notice that decreasing the increment size (Figure 7) confines the instability to a smaller region in time and decreases its amplitude. In both cases the instability dies out in a small fraction of the relaxation time and is insignificant in the sheath region at all times.

In Figure 8, the constant density contours in space and time give some idea of the lag in the response of the ions. The dashed line represents the position of the 1/e value (sheath) in space and time.

Some additional comments should be made about the error involved in the time-dependent calculations. This is a result of both the numerical method and the computing machine used. Recall from the APPLICATION OF NUMERICAL METHODS section that the modified Euler method used herein is an approximation of the Taylor series where terms of h^3 or higher are dropped. Hence, to have good accuracy, the increment, h, must be made much less than unity. Therefore, in the present case, ΔT and Δy must be small, but,

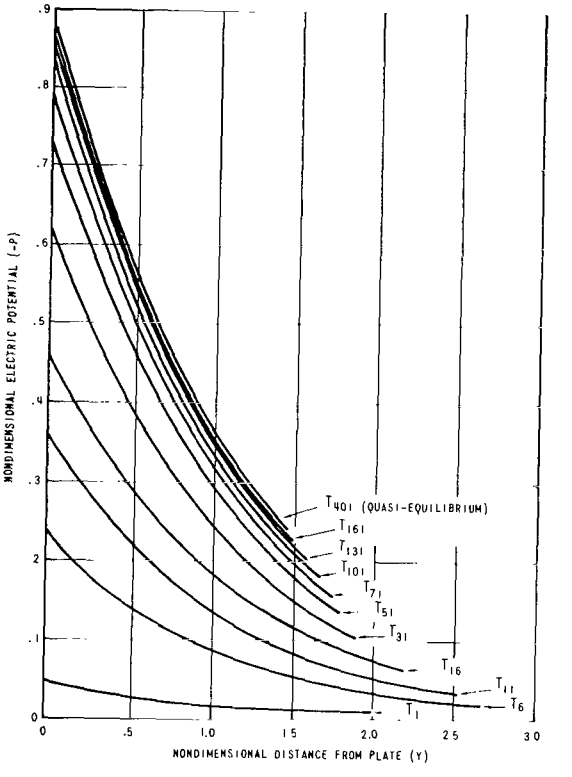

Figure 5. Growth of electric potential in space at 200 km.

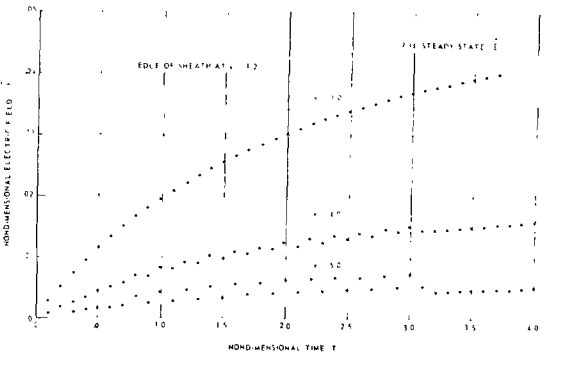

Figure 6. Time dependence of the electric field for $\Delta y = 0.1$ and $\Delta T = 0.01$ at 200 km.

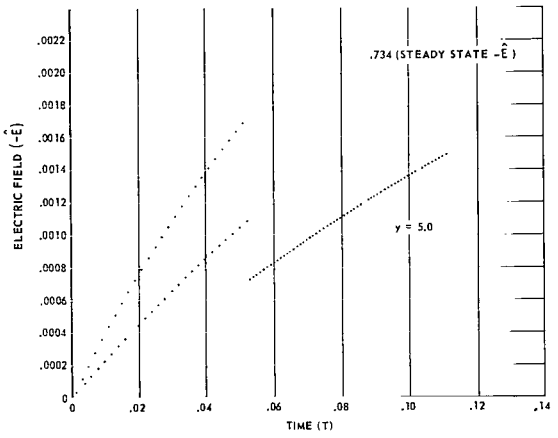

Figure 7. Time dependence of the electric field for $\Delta y = 0.01$ and $\Delta T = 0.001$ at 200 km.

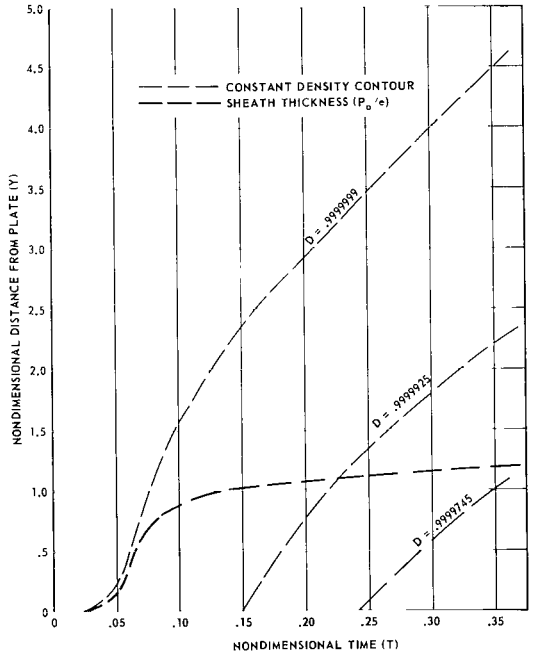

Figure 8. Constant ion density contours at 200 km.

in addition, we must satisfy the criteria for stability given in equation (27). Therefore, for an accurate, stable solution, we must have $\Delta T < \Delta y << 1$.

The above conditions, unfortunately, could not be completely complied with on the particular computing machine used. Smaller increments require a greater number of iterations, which in turn require more computer time. It was therefore necessary to use the rather large increments, $\Delta y = 0.1$ and $\Delta T = 0.01$.

The effect of using these increments can be seen if we consider the order of the terms dropped, h^3, and the number of iterations. The missing terms are on the order of 0.001 in space and 0.000001 in time. The number of iterations required in space and time are 100 and 400, respectively. Hence, from this source alone, the accumulated error at equilibrium is on the order of 0.1 and 0.0004 for the two dimensions. This, coupled with machine roundoff error (which, using standard error analysis, has an accumulated value on the order of 0.0001) can easily account for the discrepancies in the quasi-equilibrium and steady-state solutions.

SOLUTION OF CASE II

Application of Equations and Boundary Conditions

This second case treats the problem of a plate that is initially in equilibrium with the streaming plasma for a given set of physical parameters. The plasma parameters then undergo a step change. The time-dependent equations derived in the DERIVATION OF EQUATIONS section are invoked to investigate the nature of the interaction that follows as the plate adjusts to the new plasma environment.

This problem is described by the same set of time-dependent equations as Case I; namely equations (11), (12), and (13). For convenience, the physical constants corresponding to an altitude of 200 km and the steady-state distribution of the plasma parameters found in Case I are used as the boundary condition for this case at $t = 0$. After

the step change, the physical constants and plasma parameters corresponding to an altitude of 3000 km are used (Table 3). We still require that at an

TABLE 3. CASE II PARAMETERS

Symbol	Parameter	Value
-	Altitude[a] (km)	3000
N	Ion-Electron Density[a] (m^{-3})	7×10^9
T_e	Temperature[a] (K°)	4000
m_i	Average Ion Mass[a] (Amu)	4
$\bar{u}$	Average Electron Velocity[b] (km/sec)	96.2
V_s	Satellite Velocity[a] (km/sec)	6.520
L	Debye Length[b] (cm)	5.2166
ξ	Potential Factor[b] (volt/m)	6.6073
τ	Time Factor[b] (sec)	8.00×10^{-6}

a. From Table 1

b. Calculated Values

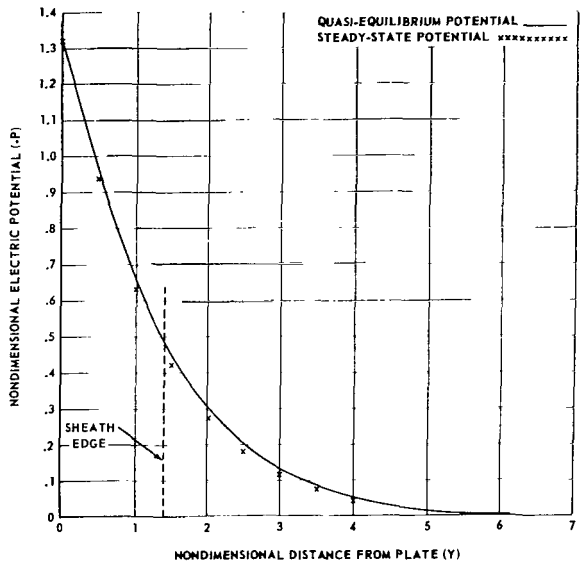

Figure 9. Spatial distribution of electric potential at 3000 km.

infinite distance from the plate, the electric field vanish, the nondimensional ion velocity and density be unity, and at the surface of the plate, the electric field be given by equation (14).

The steady-state equations can be used as in Case I to obtain the equilibrium values of the first plasma state directly. This will provide the initial boundary conditions at $t = 0$ in a form that can be fed directly into the program for the time-dependent equations.

The program for the solution of this case, which is a combination of the steady-state and time-dependent programs used in the previous chapter, is provided in Appendix C. Its operation is described sufficiently there.

Case II Results

The curve and data points given in Figure 9 represent the quasi-equilibrium ($t = 30.5\ \mu s$) and steady-state solutions for the electric potential respectively. A comparison of these results shows good agreement between the time-dependent and steady-state solutions for this case. Note that the electric potential has a greater magnitude than in Case I. Further, we find the sheath thickness to be 7.3 cm, which is also greater than in Case I. Therefore the effect of increasing the satellite altitude from 200 to 3000 km has apparently been to magnify the sheath dimension.

The time and spatial distribution of the ion density and velocity are given in Figure 10. The quasi-equilibrium solutions are represented by curves and the steady-state solutions by data points. These parameters show much better agreement than in the previous case (Figure 3). This is probably because the transition in the plasma parameters is less drastic. Note that the change in ion density and velocity near the plate is about 50 times greater than in Figure 3. This would be expected since we have already observed the electric field and electric potential to be considerably greater in this case.

The effect of varying increment size on the spatial behavior of ion density and velocity is shown in Figure 11 for $T = 0.35$. Figure 12 shows the same effect in time for the ion density and velocity at the plate ($y = 0$). Notice that in Figures 3 and 10, the quasi-equilibrium solution decreases at a

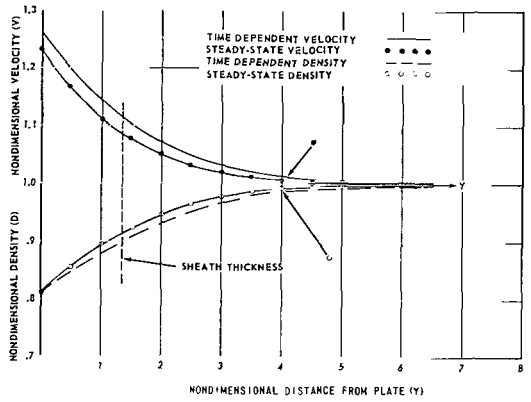

Figure 10. Ion density and velocity spatial distribution at 3000 km.

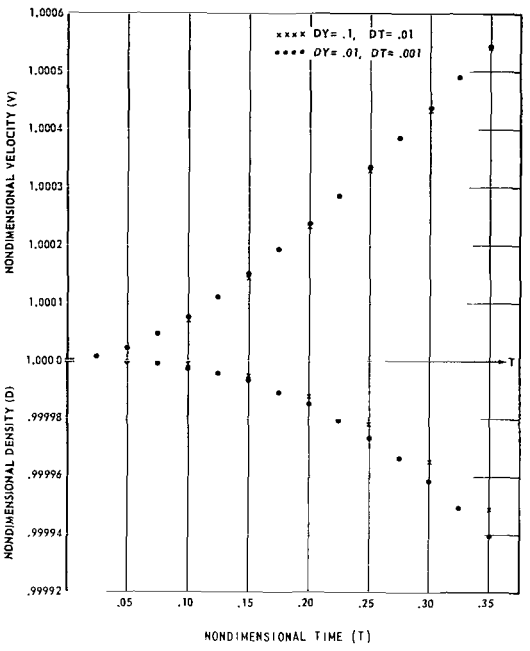

Figure 12. Effect of increment size on accuracy of time dependence.

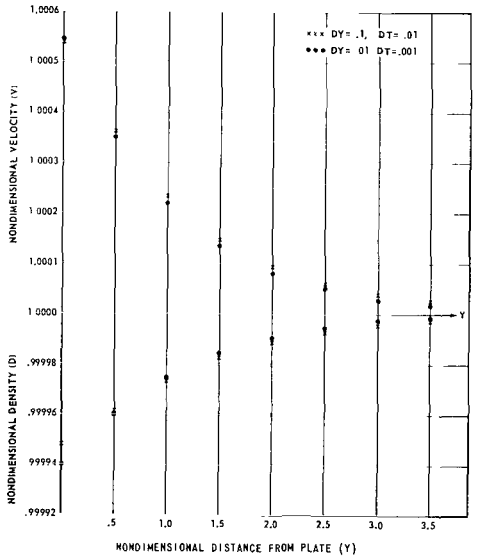

Figure 11. Effect of increment size on accuracy of spatial distribution.

slower rate than the steady-state solution. From Figure 11 it is apparent that one effect of reducing increment size is to increase the rate at which the time-dependent solutions decrease in space, thus tending to compensate for this discrepancy. The data shown in Figure 11 occurs rather early in the interaction ($T = 0.35$) so that the end effect on the quasi-equilibrium solution ($T \quad 3.81$) must be extrapolated. However, Figure 12 indicates that the effect of the decreased increment size will be more pronounced as the interaction progresses.

The time dependence of the surface charge density on the plate (Fig. 13) indicates an interesting effect not observed in Case I. The surface charge density does not increase uniformly toward equilibrium as expected, but begins to decrease after an overshoot early in the interaction. The overshoot of surface charge density, which reaches its peak value at $T = 0.8$, is the result of the electron interaction. The surface charge then begins to decrease slowly from the peak value as some of the negative charge on the plate is

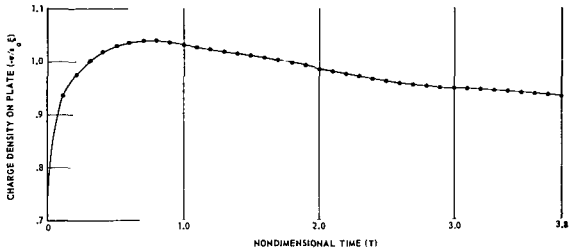

Figure 13. Growth of surface charge on plate at 3000 km.

effectively neutralized by the ions. The inertia of the ions is well demonstrated by this effect.

Figures 14 and 15 give the time dependence of the electric field very early in the interaction at various spatial positions. The fluctuations at large distances from the plate that were observed in Case I (Fig. 6) are not found here; however, there is a slight overshoot at $y = 4.1$ and $y = 5.1$. Probably, whether merely an overshoot or fluctuations are observed depends upon the magnitude of the step functions used to represent changes in plasma parameters. The gradual decrease late in the interaction is caused by ions, as previously discussed. In Figure 14 we see, however, that the point in time at which the electric field achieves its maximum value varies with distance from the plate. Apparently, the ions nearest the plate, which are consequently

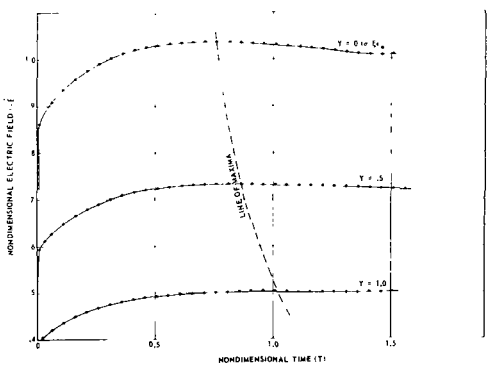

Figure 14. Growth of electric field at $y = 0.5$ and $y = 1.0$ at 3000 km.

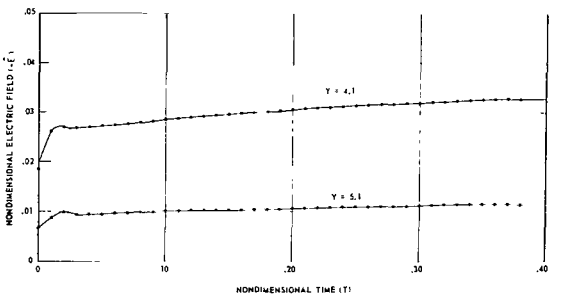

Figure 15. Growth of electric field at $y = 4.1$ and $y = 5.1$ at 3000 km.

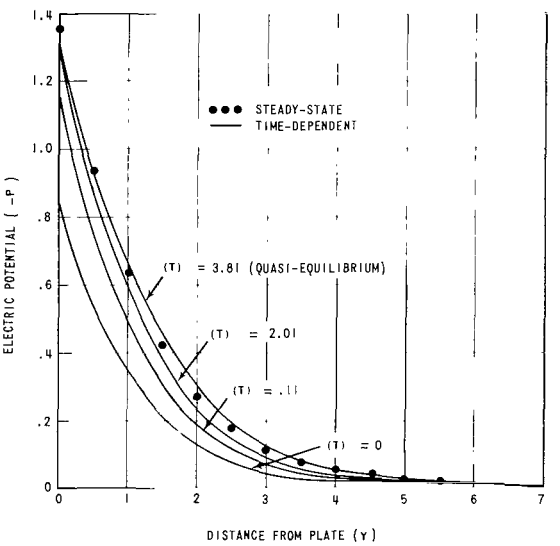

Figure 16. Growth of electric potential in space for transition from 200- to 3000-km orbit.

exposed to the greatest electric potential, experience an acceleration earlier than ions located farther away. Hence the effect of the ions is felt later at increasing distance from the plate.

Figure 16 gives the spatial dependence of the electric potential at various stages of the interaction, thus showing the approach of the solution to equilibrium.

DISCUSSION

Summary

To gain some insight into the behavior of the ionospheric plasma directly ahead of the stagnation point on a satellite, a kinetic treatment of the problem was carried out, based on two uncoupled, collisionless Boltzmann equations, corresponding to the two ionospheric species considered (ions and electrons). The formulation of this treatment of the problem was based on the assumption of an infinite, flat, conducting plate representation of the satellite; a uniform ion velocity distribution in time and space; a Maxwellian distribution of electron velocity; and an instantaneous relaxation of the electrons. With these assumptions, the equations of transport derived from the two Boltzmann equations and a form of Gauss' law were used to obtain a set of four coupled differential equations which can be solved numerically to obtain the time-dependent plasma parameters.

The first case to which these equations were applied consists of a grounded, conducting plate oriented perpendicularly to the plasma flow, which is allowed to float electrically at time t_0. The reaction resulting as the plate moves toward an equilibrium state with the plasma is very similar to the type of reaction that occurs on board satellites when the potential at some point on the surface is periodically pulsed off and on by instrumentation, such as an emissive plasma probe.

The second case, for which a solution was obtained, treats the problem in which the plate is initially taken to be at some preestablished equilibrium state. At time t_0, the plasma parameters undergo a step change and a time-dependent interaction follows as the plate moves toward a new equilibrium state compatible with its new plasma environment.

This case is particularly applicable to the behavior of the sheath region ahead of a satellite as it passes over the terminator; through a radiation belt or anomaly; or, within certain limits, undergoes a change in orbital attitude [22].

Conclusions

The results of the two cases discussed above enable us to state the major events and parameters of the time-dependent interaction and to draw the following conclusions:

a. The plasma sheath thickness changes from 0.33 cm at 200 km to 7.3 cm at 3000 km. At 200 km the sheath grows from zero when the plate is grounded to its equilibrium value in 1.42 μs, whereas the transition from equilibrium at 200 km to an equilibrium state at 3000 km requires 30.5 μs. This would indicate that the relaxation time is inversely proportional to the plasma flux to the plate (both satellite velocity and plasma density decrease in the transition from 200 km to 3000 km).

b. When plasma parameters were varied stepwise, an initial overshoot was observed in the response of the plasma sheath and surface change on the plate. This overreaction of the plasma occurred very early and dampened out quickly, permitting the plate to continue toward equilibrium in a steady manner.

c. One further event, which occurred before equilibrium was attained, is worth noting. The surface charge on the plate reached a peak negative value, 6.4 μs, after the step transition from parameters at 200 km to those at 3000 km initiated the interaction. From this point, the surface charge moved toward an equilibrium value of less magnitude. This event illustrates the delay in the response of the ions and their influence on the interaction.

d. The equilibrium potential on the plate was found to be 0.06 V at 200 km and 0.46 V at 3000 km. This is seen to be in good agreement in both form ($\xi L \doteq kT_e/q$) and magnitude with the predictions of YA. L. Al'Pert et al. [23].

From the preceding discussion, it can be concluded that the general behavior of the plasma sheath directly ahead of the frontal stagnation point on a satellite is very close to that expected from physical arguments. In addition to confirming this general, qualitative behavior, the study presented here produces a more exact, quantitative description of the interaction that can be applied to many problems with interesting and physically meaningful applications.

George C. Marshall Space Flight Center
National Aeronautics and Space Administration
Marshall Space Flight Center, Alabama 35812, October 9, 1969
124-09-00-00-62

APPENDIX A

A PROGRAM FOR THE STEADY-STATE SOLUTIONS

This program is written specifically for the steady-state equations of the Steady-State Simplification section in the text. To facilitate a clear explanation of its operation, it will be divided into six parts.

The physical parameters and constants in the first portion of the program will determine the exact physical problem to be solved. Therefore, the physical plasma parameters, temperature (XT), average ion mass (XMAS), and satellite velocity (XU), must be properly assigned. The remaining parameters will be calculated from these, and the physical constants do not change.

The second portion consists of only two statements. The first calculates the electric potential on the plate, and the second determines how closely this value must be approached.

In the third part of the program, a small potential, VX1, is assumed to exist far from the plate. This potential, VX1, is defined by the first statement. The following statement defines the slope at this point, and the last statement calculates the potential at the next adjacent point.

In the fourth section, the potential is calculated at points increasingly near the plate. When a calculated value exceeds VX0, the process is terminated. If the difference between the solution and VX0 is DELT or less, the program goes to the next section; if not, VX1 is changed slightly, and the process is repeated until the proper value of the potential at the plate is achieved.

The next section merely reverses the potential and increment arrays so that the value at the plate becomes the first component.

The last section calculates the values of ion density (XN) and velocity (W) at each point and prints out the results.

```
      N=3
      NM=1
C     ******************************************************

C     PHYSICAL PARAMETERS AND CONSTANTS

C     ******************************************************
      XT=1000.
      XMAS=28.*(1.67252*10.**(-27))
      XU=8.0450*10.**3
      EM=9.1091*10.**(-31)
      XE=1.602*10.**(-19)
      XK=1.38*10.**(-23)
      XYZ=(XK*XT)/((2.)*(3.14159)*EM)
      UE=SQRT(XYZ)
      U=(UE/XU)
      EPSX=XK*XT/(XMAS*(XU**2))
C     ******************************************************

C     VXO IS THE POTENTIAL ON THE PLATE

C     ******************************************************
      VXO=(.5)*ALOG(1./U)
      DELT=.001
C     ******************************************************

C     VX1 IS SMALL POTENTIAL ASSUMED AT SOME POINT IN SPACE

C     ******************************************************
      VX1=-.00001
      SLOPX=SQRT(1.+EPSX)*VX1
      DY=.1
      YINC(1)=DY
      YINC(2)=DY
    5 CONTINUE
      V(1)=VX1
      V(2)=SLOPX*DY+V(1)
C     ******************************************************

C     THE FOLLOWING PROGRAM EXPANDS THE SOLUTION BACK TOWARD
C     THE PLATE UNTIL VXO IS REACHED.

C     ******************************************************
      I=1
   10 CONTINUE
```

```
      YINC(I+2)=DY
      V(I+2)=2.*V(I+1)+(DY**2)*EXP(V(I+1))-(DY**2)
     1/SQRT(1.-2.*EPSX*V(I+1))-V(I)
      DIFX=ABS(VX0-V(I+2))
      IF(DIFX-DELT) 30,30,15
   15 CONTINUE
      DIFX=VX0-V(I+2)
      IF(DIFX) 16,16,20
   16 CONTINUE
      I=I+1
      GO TO 10
   20 CONTINUE
      VX1=VX1-.000005
      GO TO 5
C     ******************************************************

C     ARRAY IS REVERSED TO MAKE V(1)=VX0

C     ******************************************************
   30 MM=I+2
      MID=(MM+1)/2
      DO 40 J=1,MID
      K=MM+1-J
      TT=YINC(J)
      YINC(J)=YINC(K)
      YINC(K)=TT
      T=V(J)
      V(J)=V(K)
   40 V(K)=T
      M=MM
C     ******************************************************

C     ION DENSITY AND VELOCITY ARE CALCULATED

C     ******************************************************
      DO 60 I=1,M
      XN(I)=1./SQRT(1.-2.*EPSX*V(I))
   60 W(I)=1./XN(I)
      WRITE(N,70) (I,YINC(I),V(I),XN(I),W(I),I=1,M,NM)
   70 FORMAT(6X*INCREMENT      POTENTIAL          REL. DENSITY
     1          REL. VELOCITY*////(I6,F9.5,3E19.7))
      STOP
      END
```

APPENDIX B

A PROGRAM FOR THE CASE I TIME-DEPENDENT SOLUTION

The program that follows is designed to solve the time-dependent equations of the Nondimensional Time-Dependent Equations section in the text. It is divided into six sections.

The first section contains the various constants that determine step size and allowable error. Of particular interest are the constants DY and DT, which determine the space and time increment sizes respectively. Other constants of interest are: M, which determines how many values in the space curves are printed; MM, which determines the array size; DELP, DELD, and DELV, which are the allowable errors in the potential, ion density, and ion velocity solutions respectively; and LL, which determines how many of the time steps will be printed out.

The second section consists of the appropriate values of the plasma parameters and physical constants. The values of the factors used to nondimensionalize the variables are also calculated in this section and printed out. The names of these values are self-explanatory.

The third section sets the initial conditions of the electric field, ion density, and velocity. These values form the first set of variables in time and are fed directly into the fourth section, which is set up to calculate the first two values of each time array. As pointed out in the APPLICATION OF NUMERICAL METHODS section, the first two values cannot be calculated by many of the more accurate numerical methods.

Section five contains the bulk of the program. Here the remaining values of the array are calculated and tested for convergence in space. The first value in the electric field array is then printed, and the solution moves to the next time increment.

Section six contains the test for convergence in time and all the print statements for the variable arrays. Every LLth time step is printed out, plus whatever step the solution converges on. The convergence criteria in this section will not be satisfied unless E, D, and V have reached certain minimum differences in time.

CASE I. TIME-DEPENDENT PROGRAM

```
DIMENSION E(100,2),D(100,2),V(100,2),P(100)
*********************************************************

SECTION 1

*********************************************************
N=6
DY=.01
DT=.001
M=10
MM=100
DEL=1.*10.**(-8)
JIM=0
DELP=.00001
DIFP=DELP+1.
DELD=.000001
DELV=.000001
KK=1
JJ=10
J=JJ-1
LL=5
L=0.
ES1=0.
ES0=0.
W=1.
*********************************************************

SECTION 2

*********************************************************
XK=1.38054*10.**(-23)
T=800.
EM=9.1091*10.**(-31)
XIM=24.*(1.67252*10.**(-27))
VS=7.780*10.**(3)
EVR=(XK*T)/((2.)*(3.14159)*EM)
VA=SQRT(EVR)
ALPHA=(XK*T)/(XIM*(VS**2))
U=(VA/VS)
XNN=5.*10.**(11)
EPS=8.8542*10.**(-12)
Q=1.6021*10.**(-19)
XYZ=EPS*XK*T/((Q**2)*XNN)
XL=SQRT(XYZ)
```

```
      SQUIG=Q*XNN*XL/EPS
      DTT=DT*XL/VS
      DX=DY*XL
      WRITE(N,1) XL,SQUIG,DTT,DX,VA
    1 FORMAT(2X,3HXL=,E14.5,3X,6HSQUIG=,E14.5,3X,4HDTT=,E14.5,3X,3HDX=,
     1E14.5,3X,3HVA=,E14.5)
      ******************************************************

      SECTION 3

      ******************************************************
      DO 10 I=1,MM
      E(I,1)=0.
      D(I,1)=1.
   10 V(I,1)=1.
      ******************************************************

      SECTION 4

      ******************************************************
   20 E(1,2)=E(1,1)+(D(1,1)*V(1,1)-U*EXP(2.*ES1*DY))*DT
   22 CONTINUE
      D(1,2)=D(1,1)+D(1,1)*(V(2,1)-V(1,1))*(DT/DY)+V(1,1)*(D(2,1)-D(1,1)
     1)*(DT/DY)
      V(1,2)=V(1,1)+V(1,1)*(V(2,1)-V(1,1))*(DT/DY)-ALPHA*E(1,1)*DT
      E1=E(1,2)*(.0001)
      EE=E(1,2)
      I=1
      IF(KK-2) 24,26,26
   24 CONTINUE
      APROX=0.
      GO TO 28
   26 CONTINUE
      APROX=ES1+(ES1-ES0)
   28 CONTINUE
      ES2=-ABS(APROX-EE)
      E(I+1,2)=E(I,2)+(D(I,2)-EXP(ES2*DY))*DY
      EE=EE+(E(I+1,2)-E(I,2))/2.+E(I+1,2)
      I=I+1
      D(I,2)=(D(I-1,1)+D(I+1,1))/2.+(D(I,1)*(V(I+1,1)-V(I-1,1))+V(I,1)*
     1(D(I+1,1)-D(I-1,1)))*DT/(2.*DY)
      V(I,2)=(V(I-1,1)+V(I+1,1))/2.+V(I,1)*(V(I+1,1)-V(I-1,1))*DT/
     1(2.*DY)-ALPHA*(E(I-1,1)+E(I+1,1))*DT/2.
   30 CONTINUE
      ******************************************************

      SECTION 5

      ******************************************************
      ES2=-ABS(APROX-EE)
      E(I+1,2)=E(I-1,2)+2.*(D(I,2)-EXP(ES2*DY))*DY
      TEST=E(I+1,2)
      IF(TEST) 34,34,32
   32 CONTINUE
```

```
      E(I+1,2)=0.
   34 CONTINUE
      EE=EE+(E(I+1,2)-E(I,2))/2.+E(I+1,2)
      I=I+1
      TEST=E(I+1,1)
      IF(TEST) 36,35,36
   35 CONTINUE
      D(I,2)=1.
      V(I,2)=1.
      GO TO 38
   36 CONTINUE
      D(I,2)=(D(I-1,1)+D(I+1,1))/2.+(D(I,1)*(V(I+1,1)-V(I-1,1))+V(I,1)*
     1(D(I+1,1)-D(I-1,1)))*DT/(2.*DY)
      V(I,2)=(V(I-1,1)+V(I+1,1))/2.+V(I,1)*(V(I+1,1)-V(I-1,1))*DT/
     1(2.*DY)-ALPHA*(E(I-1,1)+E(I+1,1))*DT/2.
   38 CONTINUE
      NN=MM-1
      IF(I-NN) 40,50,50
   40 CONTINUE
      GO TO 30
   50 CONTINUE
      E(I+1,2)=E(I-1,2)+2.*(D(I,2)-EXP(FS2*DY))*DY
      TEST=E(I+1,2)
      IF(TEST) 56,56,54
   54 CONTINUE
      E(I+1,2)=0.
   56 CONTINUE
      EE=EE+(E(I+1,2)-E(I,2))/2.+E(I+1,2)
      D(I+1,2)=D(I,2)
      V(I+1,2)=V(I,2)
      MM=I+1
      DIFA=ABS(APROX-EE)
      DELT=ABS(EE*.01)
      IF(DIFA-DELT) 70,70,60
   60 CONTINUE
      DIFA=(APROX-EE)
      APROX=APROX-DIFA/W
      W=W+.5*W
      I=1
      EE=E(1,2)
      GO TO 28

   70 CONTINUE
      W=1.5
      WRITE(N,80) KK,E(1,2)
   80 FORMAT(6X,22HELECTRIC FIELD AT TIME,2X,I4,2X,7HE(1,2)=,E14.5)
      **********************************************************

      SECTION 6

      **********************************************************
      L=L+1
      IF(L-LL) 85,85,84
   84 CONTINUE
```

```
      DIFP=ABS(EE-ES1)
      DIFD=ABS(D(1,2)-D(1,1))
      DIFV=ABS(V(1,2)-V(1,1))
      IF(DIFP-DELP) 300,300,85
  300 CONTINUE
      IF(DIFD-DELD) 310,310,85
  310 CONTINUE
      IF(DIFV-DELV) 90,90,85
   85 CONTINUE
      J=J+1
      IF(J-JJ) 160,90,90
   90 CONTINUE
      J=0
      WRITE(N,100) KK
  100 FORMAT(//2X,25HPLASMA PARAMETERS AT TIME,2X,I4)
      NN=MM-1
      SUM=EE
      DO 110 I=1,NN
      P(I)=SUM*DY
      SUM=SUM-(E(I,2)+E(I+1,2))/2.
      IF(SUM) 110,110,104
  104 CONTINUE
      SUM=0.
  110 CONTINUE
      P(MM)=P(NN)
      WRITE(N,120) (I,P(I),I=1,MM,M)
  120 FORMAT(///2X,9HPOTENTIAL//(6X,I6,E16.7,I6,E16.7,I6,E16.7,I6,E16.7,
     1I6,E16.7))
      WRITE(N,130) (I,E(I,2),I=1,MM,M)
  130 FORMAT(///2X,14HELECTRIC FIELD//(6X,I6,E16.7,I6,E16.7,I6,F16.7,I6,
     1E16.7,I6,F16.7))
      WRITE(N,140) (I,D(I,2),I=1,MM,M)
  140 FORMAT(///2X,18HION NUMBER DENSITY//(6X,I6,E16.7,I6,E16.7,I6,F16.7
     1,I6,E16.7,I6,E16.7))
      WRITE(N,150) (I,V(I,2),I=1,MM,M)
  150 FORMAT(///2X,20HAVERAGE ION VELOCITY//(6X,I6,E16.7,I6,E16.7,I6,
     1E16.7,I6,F16.7,I6,E16.7))
      WRITE(N,155)
  155 FORMAT(///)
      IF(L-LL) 160,160,156
  156 CONTINUE
      IF(DIFP-DELP) 320,320,330
  320 CONTINUE
      WRITE(N,315)
  315 FORMAT(3X,11HP CONVERGES/)
      JIM=JIM+1
  330 CONTINUE
      IF(DIFD-DELD) 340,340,350
  340 CONTINUE
      WRITE(N,345)
  345 FORMAT(3X,11HD CONVERGES/)
      JIM=JIM+1
  350 CONTINUE
      IF(DIFV-DELV) 360,360,160
```

```
360 CONTINUE
    WRITE(N,365)
365 FORMAT(3X,11HV CONVERGES/)
    JIM=JIM+1
    IF(JIM-3) 160,190,190
160 CONTINUE
    DO 180 I=1,MM
    E(I,1)=E(I,2)
    D(I,1)=D(I,2)
180 V(I,1)=V(I,2)
    ES0=ES1
    ES1=FE
    EE=0.
    KK=KK+1
    JIM=0
    GO TO 20
190 CONTINUE
    WRITE(N,200)
200 FORMAT(2X,22HEQUILIBRIUM CONDITIONS)
    STOP
    END
```

APPENDIX C

A PROGRAM FOR THE CASE II TIME-DEPENDENT SOLUTION

The program in this appendix is designed to solve the general time-dependent problem treated in case II. In this form, the program can solve the time-dependent equations developed in the DERIVATION OF EQUATIONS section for any of the various applications pointed out in the DISCUSSION. The program is divided into two sections for the following discussion.

The first section essentially consists of a revised form of the program presented in Appendix A. Here the variable arrays, which were one-dimensional in Appendix A, are written in a two-dimensional form so that they can be applied directly to the time-dependent portion of the program in the form of initial conditions. In this first section, the physical constants and plasma parameters constitute the initial conditions, or the initial plasma state. The constants and plasma parameters at the first of section two will constitute the final plasma state.

The second section of this program is almost identical to the program presented in Appendix B. Therefore, we will point out and explain the differences in the two here.

The form and purpose of the various constants are the same here as in Appendix A. However, the values of the plasma parameters have been changed in order to formulate the problem described in the SOLUTION OF CASE II section.

The part of the program referred to as section two in Appendix B has been omitted here. This section provided the boundary conditions, which are calculated in section one of this program.

The remainder of the program is identical to that presented in Appendix B and will therefore not be discussed further here.

CASE II. TIME-DEPENDENT PROGRAM

```
      DIMENSION YINC(1000)
      DIMENSION E(1000,2),D(1000,2),V(1000,2),P(1000)
      ******************************************************

      SECTION 1

      ******************************************************

      PLASMA STATE 1 PARAMETERS

      N=6
      M=10
      KK=0
      XU=7.78*10.**(3)
      XT=800.
      EM=9.1091*10.**(-31)
      XE=1.602*10.**(-19)
      XK=1.38*10.**(-23)
      XMAS=24*(1.67252*10.**(-27))
      DELT=.001
      EPSX=XK*XT/(XMAS*(XU**2))
      DO=1.
      VO=1.
      XYZ=(XK*XT)/((2.)*(3.14159)*EM)
      UE=SQRT(XYZ)
      U=(UE/XU)
      VXO=(.5)*ALOG(1./U)
      VX1=-.00005
 1009 CONTINUE
      SLOPX=SQRT(1.+EPSX)*VX1
      DY=.1
      DO 1001 I=1,110
      P(I)=0.
 1001 CONTINUE
      P(1)=VX1
      P(2)=SLOPX*DY+P(1)
      I=1
 1010 CONTINUE
      YINC(I+2)=DY
      P(I+2)=2.*P(I+1)+(DY**2)*EXP(P(I+1))-(DY**2)/SQRT(1.-2.*EPSX
     1*P(I+1))-P(I)
      DIFX=ABS(VXO-P(I+2))
      IF(DIFX-DELT) 1030,1030,1015
```

```
1015 CONTINUE
     DIFX=VX0-P(I+2)
     IF(DIFX) 1016,1016,1020
1016 CONTINUE
     I=I+1
     GO TO 1010
1020 CONTINUE
     VX1=VX1-.000001
     GO TO 1005
1030 MM=I+2
     MID=(MM+1)/2
     DO 1040 J=1,MID
     K=MM+1-J
     TT=YINC(J)
     YINC(J)=YINC(K)
     YINC(K)=TT
     T=P(J)
     P(J)=P(K)
1040 P(K)=T
     DO 1060 I=1,MM
     V(I,1)=SQRT(1.-2.*EPSX*P(I))
1060 D(I,1)=1./V(I,1)
     WRITE(N,12) KK
  12 FORMAT(//2X,25HPLASMA PARAMETERS AT TIME,2X,I4)
     ********************************************************

     SECTION 2

     ********************************************************

     PLASMA STATE 2 PARAMETERS

     DY=10.
     DT=.001
     MM=800
     DEL=1.*10.**(-8)
     JIM=0
     DELP=.005
     DELD=.000001
     DELV=.000001
     L=0
     LL=5
     KK=1
     JJ=10
     J=JJ-1
     ES1=0.
     ES0=0.
     W=1.

     XK=1.38054*10.**(-23)
     T=4000.
     EM=9.1091*10.**(-31)
```

```
      XIM=4.*(1.67252*10.**(-27))
      VS=6.520*10.**(3)
      EVR=(XK*T)/((2.)*(3.14159)*EM)
      VA=SQRT(EVR)
      ALPHA=(XK*T)/(XIM*(VS**2))
      U=(VA/VS)

      XNN=7.*10.**(9)
      EPS=8.8542*10.**(-12)
      Q=1.6021*10.**(-19)
      XYZ=EPS*XK*T/((Q**2)*XNN)
      XL=SQRT(XYZ)
      SQUIG=Q*XNN*XL/EPS
      DTT=DT*XL/VS
      DX=DY*XL
      WRITE(N,1) XL,SQUIG,DTT,DX
    1 FORMAT(2X,3HXL=,E14.5,3X,6HSQUIG=,E14.5,3X,4HDTT=,E14.5,3X,3HDX=,
     1E14.5)

      WRITE(N,16) (I,P(I),I=1,MM,M)
   16 FORMAT(///2X,9HPOTENTIAL//(6X,I6,F16.7,I6,E16.7,I6,E16.7,I6,E16.7,
     1I6,E16.7))
      I=1
      E(I,1)=-(P(2)-P(1))/DY
      DO 10 I=2,MM
      E(I,1)=-(P(I+1)-P(I-1))/(2.*DY)
   10 CONTINUE
      WRITE(N,17) (I,E(I,1),I=1,MM,M)
   17 FORMAT(///2X,14HELECTRIC FIELD//(6X,I6,E16.7,I6,E16.7,I6,E16.7,I6,
     1E16.7,I6,E16.7))
      WRITE(N,18) (I,D(I,1),I=1,MM,M)
   18 FORMAT(///2X,18HION NUMBER DENSITY//(6X,I6,E16.7,I6,E16.7,I6,E16.7
     1,I6,E16.7,I6,E16.7))
      WRITE(N,19) (I,V(I,1),I=1,MM,M)
   19 FORMAT(///2X,20HAVERAGE ION VELOCITY//(6X,I6,E16.7,I6,E16.7,I6,
     1E16.7,I6,E16.7,I6,E16.7))
      WRITE(N,1000)
 1000 FORMAT(///)

   20 E(1,2)=E(1,1)+(D(1,1)*V(1,1)-U*EXP(2.*ES1*DY))*DT
      GO TO 23
   21 CONTINUE
      E(1,2)=E(1,1)
   23 CONTINUE
      D(1,2)=D(1,1)+D(1,1)*(V(2,1)-V(1,1))*(DT/DY)+V(1,1)*(D(2,1)-D(1,1)
     1)*(DT/DY)
      V(1,2)=V(1,1)+V(1,1)*(V(2,1)-V(1,1))*(DT/DY)-ALPHA*E(1,1)*DT
      E1=E(1,2)*(.0001)
      EE=E(1,2)
      I=1
      IF(KK-2) 24,26,26
   24 CONTINUE
      APROX=0.
```

```
      GO TO 28
   26 CONTINUE
      APROX=ES1+(ES1-ES0)

   28 CONTINUE
      ES2=-ABS(APROX-EE)

      IF(V(1,2)-V(1,1)) 400,400,410
  400 CONTINUE
      E(I+1,2)=E(I+1,1)
      GO TO 420
  410 CONTINUE
      E(I+1,2)=E(I,2)+(D(I,2)-EXP(ES2*DY))*DY
  420 CONTINUE
      EE=EE+(E(I+1,2)-E(I,2))/2.+E(I+1,2)
      I=I+1
      D(I,2)=(D(I-1,1)+D(I+1,1))/2.+(D(I,1)*(V(I+1,1)-V(I-1,1))+V(I,1)*
     1(D(I+1,1)-D(I-1,1)))*DT/(2.*DY)
      V(I,2)=(V(I-1,1)+V(I+1,1))/2.+V(I,1)*(V(I+1,1)-V(I-1,1))*DT/
     1(2.*DY)-ALPHA*(E(I-1,1)+E(I+1,1))*DT/2.

   30 CONTINUE
      ES2=-ABS(APROX-EE)

      IF(V(1,2)-V(1,1)) 430,430,440
  430 CONTINUE
      E(I+1,2)=E(I+1,1)
      GO TO 450
  440 CONTINUE
      E(I+1,2)=E(I-1,2)+2.*(D(I,2)-EXP(ES2*DY))*DY
  450 CONTINUE

      TEST=E(I+1,2)
      IF(TEST) 34,34,32
   32 CONTINUE
      E(I+1,2)=0.
   34 CONTINUE
      EE=EE+(E(I+1,2)-E(I,2))/2.+E(I+1,2)
      I=I+1
      TEST=E(I+1,1)
      IF(TEST) 36,35,36
   35 CONTINUE
      D(I,2)=1.
      V(I,2)=1.
      GO TO 38
   36 CONTINUE
      D(I,2)=(D(I-1,1)+D(I+1,1))/2.+(D(I,1)*(V(I+1,1)-V(I-1,1))+V(I,1)*
     1(D(I+1,1)-D(I-1,1)))*DT/(2.*DY)
      V(I,2)=(V(I-1,1)+V(I+1,1))/2.+V(I,1)*(V(I+1,1)-V(I-1,1))*DT/
     1(2.*DY)-ALPHA*(E(I-1,1)+E(I+1,1))*DT/2.
   38 CONTINUE
      NN=MM-1
      IF(I-NN) 40,50,50
```

```
 40 CONTINUE
    GO TO 30
 50 CONTINUE

    IF(V(1,2)-V(1,1)) 460,460,470
460 CONTINUE
    E(I+1,2)=E(I+1,1)
    GO TO 480
470 CONTINUE
    E(I+1,2)=E(I-1,2)+2.*(D(I,2)-EXP(ES2*DY))*DY
480 CONTINUE
    TEST=E(I+1,2)
    IF(TEST) 56,56,54
 54 CONTINUE
    E(I+1,2)=0.
 56 CONTINUE
    EE=EE+(E(I+1,2)-E(I,2))/2.+E(I+1,2)
    D(I+1,2)=D(I,2)
    V(I+1,2)=V(I,2)
    MM=I+1
    DIFA=ABS(APROX-EE)
    DELT=ABS(EE*.01)
    IF(DIFA-DELT) 70,70,60
 60 CONTINUE
    DIFA=(APROX-EE)

    APROX=APROX-DIFA/W
    W=W+.5*W
    I=1
    EE=E(1,2)
    GO TO 28

 70 CONTINUE
    W=1.5
    WRITE(N,80) KK,E(1,2)
 80 FORMAT(6X,22HELECTRIC FIELD AT TIME,2X,I4,2X,7HE(1,2)=,E14.5)
    L=L+1
    IF(L-LL) 85,85,84
 84 CONTINUE
    DIFP=ABS(EE-ES1)
    DIFD=ABS(D(1,2)-D(1,1))
    DIFV=ABS(V(1,2)-V(1,1))
    IF(DIFP-DELP) 300,300,85
300 CONTINUE
    IF(DIFD-DELD) 310,310,85
310 CONTINUE
    IF(DIFV-DELV) 90,90,85
 85 CONTINUE
    J=J+1
    IF(J-JJ) 160,90,90
 90 CONTINUE
    J=J
    WRITE(N,100) KK
```

```
100 FORMAT(//2X,25HPLASMA PARAMETERS AT TIME,2X,I4)
    NN=MM-1
    SUM=EE
    DO 110 I=1,NN
    P(I)=SUM*DY
    SUM=SUM-(E(I,2)+E(I+1,2))/2.
    IF(SUM) 110,110,104
104 CONTINUE
    SUM=0.
110 CONTINUE
    P(MM)=P(NN)
    WRITE(N,120) (I,P(I),I=1,MM,M)
120 FORMAT(///2X,9HPOTENTIAL//(6X,I6,E16.7,I6,E16.7,I6,E16.7,I6,E16.7,
   1I6,E16.7))
    WRITE(N,130) (I,E(I,2),I=1,MM,M)
130 FORMAT(///2X,14HELECTRIC FIELD//(6X,I6,E16.7,I6,E16.7,I6,E16.7,I6,
   1E16.7,I6,E16.7))
    WRITE(N,140) (I,D(I,2),I=1,MM,M)
140 FORMAT(///2X,18HION NUMBER DENSITY//(6X,I6,E16.7,I6,E16.7,I6,E16.7
   1,I6,E16.7,I6,E16.7))
    WRITE(N,150) (I,V(I,2),I=1,MM,M)
150 FORMAT(///2X,20HAVERAGE ION VELOCITY//(6X,I6,E16.7,I6,E16.7,I6,
   1E16.7,I6,E16.7,I6,E16.7))
    WRITE(N,155)
155 FORMAT(///)
    IF(L-LL) 160,160,156
156 CONTINUE

    CONVERGANCE TEST

    IF(DIFP-DELP) 320,320,330
320 CONTINUE
    WRITE(N,315)
315 FORMAT(3X,11HP CONVERGES/)
    JIM=JIM+1
330 CONTINUE
    IF(DIFD-DELD) 340,340,350
340 CONTINUE
    WRITE(N,345)
345 FORMAT(3X,11HD CONVERGES/)
    JIM=JIM+1
350 CONTINUE
    IF(DIFV-DELV) 360,360,160
360 CONTINUE
    WRITE(N,365)
365 FORMAT(3X,11HV CONVERGES/)
    JIM=JIM+1
    IF(JIM-3) 160,190,190
160 CONTINUE
```

```
      RESET FOR NEXT TIME ITERATION

      V1=V(1,1)
      DO 180 I=1,MM
      E(I,1)=E(I,2)
      D(I,1)=D(I,2)
  180 V(I,1)=V(I,2)
      ESO=ES1
      ES1=EE
      EE=0.
      KK=KK+1
      JIM=0
      IF(V(1,2)-V1) 21,21,20
  190 CONTINUE
      WRITE(N,200)
  200 FORMAT(2X,22HEQUILIBRIUM CONDITIONS)
      STOP
      END
```

REFERENCES

1. Jastrow, R.; and Pearse, C. A.: J. Geophys. Res., vol. 62, 1957, p. 413.

2. Kraus, L.; and Watson, K.: Phys. Fluids, vol. 1, 1958, p. 480.

3. Davis, A. H.; and Harris, I.: Rarefied Gas Dynamics. Academic Press (New York), 1961, p. 661.

4. Kino, G.; Self, S.; and Pavkovitch, J.: Research on Plasma Boundary Studies. ARL-65-131, Office of Aerospace Research, U.S. Air Force (Wright-Patterson AFB, Ohio), July 1965.

5. Self, S. A.: Exact Solution of the Collisionless Plasma Sheath Equation. Phys. Fluids, vol. 6, December 1963, pp. 1762-8.

6. Harp, R.; and Kino, G. S.: Measurement of Fields in the Plasma Sheath by an Electron Beam Probing Technique. Paper presented at Sixth Int. Conf. on Ionization Phenomena in Gases (Paris), July 1963.

7. Harp, R. S.; Kino, G. S.; and Pavkovitch, J.: rf Properties of the Plasma Sheath, Phys. Rev. Letters, vol. 11, October 1963, p. 310.

8. Getmantsev, C. G.; and Denisov, N. G.: Geomagnetism and Aeronomy. vol. 2, 1962, p. 575.

9. Al'Pert, YA. L.; Gurevich, A. V.; and Pitaevskii, L. P.: Effects Produced by an Artificial Satellite Rapidly Moving in the Ionosphere or in an Interplanetary Medium. Soviet Phys. Uspekhi, vol. 6, 1963, p. 13.

10. Hall, David F.; Kemp, Robert F.; and Sellen, J. M., Jr.: Generation and Characteristics of Plasma Wind-Tunnel Streams, AIAA J., vol. 3, August 1965, pp. 1490-97.

11. Vincenti, Walter G.; and Kruger, Charles H.: Introduction to Physical Gas Dynamics. John Wiley and Sons, New York, 1965, pp. 328-333.

12. Ibid., pp. 368-374.

13. Ulman, Martin A.: Introduction to Plasma Physics. McGraw-Hill Book Company, 1964, Chap. 2.

14. Op. Cit., Vincenti and Kruger, pp. 27-47.

15. Ibid., p. 346.

16. Ibid., p. 523.

17. Reitz, John R.; and Milford, Frederick J.: Foundations of Electromagnetic Theory Addison-Wesley Publishing Company, (Reading, Mass.), 1962, pp. 31-36.

18. Scarborough, James B.: Numerical Mathematical Analysis: Fifth Edition. The Johns Hopkins Press (Baltimore, Md.), 1962, pp. 308-309.

19. Cunningham, W. J.: Introduction to Nonlinear Analysis. McGraw-Hill Book Company (New York), 1958, Chap. 2.

20. Op. Cit., Scarborough, pp. 385-401.

21. Walsh, J.: Numerical Analysis: An Introduction. Thompson Book Company, (Washington, D.C.), 1967, Chap. 6.

22. Application is limited at an upper level by the ratio of Debye length to body size and at a lower range by collision effects.

23. Op. Cit., YA. L. Al'Pert, et al., p. 27.

NASA-Langley, 1970 —— 25 M431

NATIONAL AERONAUTICS AND SPACE ADMINISTRATION
WASHINGTON, D.C. 20546

OFFICIAL BUSINESS

FIRST CLASS MAIL

POSTAGE AND FEES PAID
NATIONAL AERONAUTICS AND
SPACE ADMINISTRATION

"The aeronautical and space activities of the United States shall be conducted so as to contribute . . . to the expansion of human knowledge of phenomena in the atmosphere and space. The Administration shall provide for the widest practicable and appropriate dissemination of information concerning its activities and the results thereof."

—NATIONAL AERONAUTICS AND SPACE ACT OF 1958

NASA SCIENTIFIC AND TECHNICAL PUBLICATIONS

TECHNICAL REPORTS: Scientific and technical information considered important, complete, and a lasting contribution to existing knowledge.

TECHNICAL NOTES: Information less broad in scope but nevertheless of importance as a contribution to existing knowledge.

TECHNICAL MEMORANDUMS: Information receiving limited distribution because of preliminary data, security classification, or other reasons.

CONTRACTOR REPORTS: Scientific and technical information generated under a NASA contract or grant and considered an important contribution to existing knowledge.

TECHNICAL TRANSLATIONS: Information published in a foreign language considered to merit NASA distribution in English.

SPECIAL PUBLICATIONS: Information derived from or of value to NASA activities. Publications include conference proceedings, monographs, data compilations, handbooks, sourcebooks, and special bibliographies.

TECHNOLOGY UTILIZATION PUBLICATIONS: Information on technology used by NASA that may be of particular interest in commercial and other non-aerospace applications. Publications include Tech Briefs, Technology Utilization Reports and Notes, and Technology Surveys.

Details on the availability of these publications may be obtained from:

SCIENTIFIC AND TECHNICAL INFORMATION DIVISION

NATIONAL AERONAUTICS AND SPACE ADMINISTRATION

Washington, D.C. 20546